Chapter 8: Characterization of optimized formulation

8.0 Characterization of Optimized formulation

8.1 Introduction

Various attempts have been made to improve the clinical safety and efficiency of the therapeutic standard Doxil™ and its generic equivalent Lipodox™. The drug regulatory agencies United states food and drug administration (USFDA) and European Medicines Agency (EMA) have identified liposomal formulations as complex injectables requiring thorough characterization using various techniques to ascertain effect of various components on the physico-chemical properties and stability of such formulations. These properties have been correlated to the PK-PD profiles of the formulations and their clinical effectiveness. Further, design of the liposomal formulation requires the modulating the surface characteristics in appropriate way to present the intact nanocarrier to the intended target cells. Consequently, the USFDA and EMA have published reflection papers as well as general guidance on liposomal formulations along with product specific ones for the development of generic equivalents of innovator products (1, 2). The optimized dual drug formulation was characterized using various orthogonal techniques to evaluate the effect of the Vincristine co-loading in the PEGylated liposomal Doxorubicin. The physico-chemical characterization and their intended usage have been detailed in Table 19.

Sl. No	Physico-chemical characterization test	Intended uses
1	Quantification of drugs and lipids by Reverse phase High performance liquid chromatography (RP-HPLC)	Estimation of the entrapment efficiency and the loading capacity of the drugs in the liposomes
2	Particle size and Zeta Potential using Zetasizer	Hydrodynamic diameter and surface potential of the liposomes
3	Attenuated Total reflection - Fourier transform infrared spectroscopy	Interaction potential of the active pharmaceutical ingredients with the excipients. The region of localization of the drugs in the liposomes.
4	Microcalorimetry	Thermotropic behaviour of the optimized liposomal formulations, interaction potential of the drugs with the lipid bilayer.

Sl. No	Physico-chemical characterization test	Intended uses
5	Cryogenic-Transmission electron microscopy (TEM)	External and internal morphology, size of the liposomes, lamellarity of the liposomes, strand thickness of the DOX nanoprecipitates
6	Atomic force microscopy (AFM) and Field emission scanning electron microscopy (FESEM).	External surface morphology and particle size.
7	Fixed aqueous layer thickness (FALT) study	The grafted PEG layer thickness /fixed aqueous layer associated with the optimized liposomal formulation
8	Electrolyte-induced flocculation/aggregation	The uniformity and stability of the pegylation chains on surface of the liposomes.
9	Interaction with Serum proteins and protein adsorption	In-vivo stability of the formulations in serum and proteins on circulation in blood.
10	Plasma Stability study	Effect of long circulation on the particle size and entrapment efficiency of the drugs in the liposomes.
11	Liposome Membrane Integrity test	Effect of cholesterol in the composition and to determine whether dual loading in the liposomes has any significant impact on the lipid structures integrity
12	Small Angle X-ray scattering (SAXS)	Structural parameters of liposomes like particle size, morphology, aggregation potential, degree of disorderliness, effect of drug loading into liposomes. The region of localization of the drugs in the liposomes.
13	In-vitro drug release study	Drug release from the formulated liposomes under the conditions which these carriers may encounter in normal tissues (pH 7.4), cancerous tissues (pH 6.4) and inside the cancerous cells (pH 5.5). Drug release in presence of biological fluids (dilution induced release).
14	Haemolysis Study	The extent of physiological compatibility post administration of formulation into the blood and toxicity of formulations to RBC
15	Stability Study	Assessment of storage temperature on the CQAs and determination of shelf life.

Table 19: List of the evaluated physico-chemical properties of the optimized formulation

8.2 Materials

The drugs, Vincristine sulphate (VCR) and Doxorubicin Hydrochloride (DOX) were procured from Minakem (France) and Synbias Pharma Ltd (Ukraine) respectively. The lipids fully hydrogenated soy phosphatidylcholine (HSPC) and 1,2-distearoyl-sn-glycero-3-

phosphoethanolamine-N-[methoxy(polyethyleneglycol)2000] (mPEG-DSPE) were obtained from Lipoid GmbH (Switzerland). Cholesterol was procured from Dishman Netherlands BV (Netherlands). Ammonium sulphate, histidine and sucrose were purchased from Merck KGaA (Germany). Ethyl Alcohol was purchased from Commercial Alcohols (Canada). All other chemicals used in the study were of HPLC grade.

8.3 Characterization of optimized formulation

8.3.1 Preparation of liposomes

Drug free Liposomes were prepared by the ethanolic injection method. The lipids HSPC, cholesterol and mpeg-2k-DSPE in 56.55:38.19:5.26 molar ratio was dissolved in ethanol by heating at 65±5°C and subsequently passively hydrated using aqueous solution of ammonium sulphate (molar concentration 350 mM) by continuous stirring at 400 rpm (2 mag systems GmBH, Germany) at 65±5°C (Julabo GmBH, Germany) for 30 minutes to form the multilamellar vesicles. The size of these vesicles was then reduced to 100±20 nm using 10 cycles of pneumatic passage at 65±5°C through 80 nm polycarbonate membrane filters stacked in a thermobarrel extruder (Northern lipids, Canada). The formed liposomal suspension was then buffer exchanged into 300 mM sucrose by tangential flow filtration (750kD MWCO, 420 cm^2 surface area, GE healthcare, Singapore) to remove the excess ammonium sulphate and aid in the creation of the transmembrane ion concentration gradient. The drugs vincristine sulphate and doxorubicin hydrochloride were then actively co-loaded into the formed vesicles by the ammonium ion gradient. Briefly the drugs in determined synergistic weight ratio (VCR: DOX 1:2) was dissolved in the 300 mM sucrose and added to the pH adjusted liposomal suspension (pH 5.5 using 1.5 mM histidine) maintained at 65±5°C with continuous stirring at 400 rpm for 60 minutes.

The ensuing physico-chemical characterization studies was performed using formulations of drug free liposomes, vincristine liposomes, doxorubicin liposomes and dual drug liposomes prepared using above mentioned manufacturing process. The preformed liposomes dissolved in 300 mM sucrose was adjusted to pH 5.5 using 1.5 mM histidine buffer and resulting formulation was used as drug-free liposomes. The single drug loaded doxorubicin liposomes

and vincristine liposomes were prepared by incubating the pH adjusted preformed liposomes with drug solutions using the aforementioned conditions of active loading.

8.3.2 Quantification of drugs in optimised liposomes

The content of Doxorubicin hydrochloride (DOX) and Vincristine hydrochloride (VCR) was simultaneously determined using reverse phase High Performance Liquid Chromatography (HPLC) analysis using C18 as stationary phase as detailed in section 7.4. Briefly, the mixed standard solution of drugs was prepared using definite concentrations of the pure drugs (27 mg DOX and 13 mg VCR) and dissolving it in methanol followed by sonication (Oscar Ultrasonics, Mumbai, India) for 3 minutes. The mobile phase for gradient elution was prepared using ammonium formate solution pH 4.5 with subsequent mixing with methanol (80:20 v/v- mobile phase A) and with acetonitrile (20:80 v/v- mobile phase B). The flow rate was maintained at 1.0 mL/min by Agilent 1100 series (Agilent USA) on 3.5µ symmetry shield RP column (150 X 4.6 mm) (Waters, USA) with detection at 254 nm using UV variable wavelength detector (Agilent, Santa Clara, USA). The methanol to water mixture (50:50 v/v) was used to ensure the complete disruption of the lipid bilayer resulting in release of entire DOX and VCR into the solution with subsequent analysis of the drug content (Retention time of DOX and VCR: 4-6 minutes and 7-9 minutes respectively). The separation of the free drug from the entrapped drug was carried out by gel filtration chromatography using Superdex 75 (GE healthcare, Singapore). 0.5 ml samples were taken and added to the pre-conditioned Superdex columns with subsequent application of 2 bar positive pressure using Ezypress 48 (Orochem Technologies Inc, USA). The free drug entrapped in the cartridge was eluted using 3.0 ml of buffer solution and subsequently analysed for the content of the drugs in similar manner as mentioned above for assay. The entrapment drug content was calculated based on the values of assay of the drugs and the free drug content from the liposomal formulations using the calculated using previously reported equations (3).

$$\text{Entrapment Efficiency} = \frac{\text{Amount of drug loaded in liposomes}}{\text{Amount of drug taken for liposomes preparation}} \text{ X } 100$$

$$\text{Loading Efficiency} = \frac{\text{Amount of drug loaded in liposomes}}{\text{Amount of lipids used in liposomes}} \text{ X } 100$$

$$\text{Entrapment efficiency} = \frac{\text{(Assay of drugs- free drug content) X100}}{\text{Assay of drug}}$$

8.3.3 Quantification of lipids

The estimation of the lipids was done using RP-HPLC using method as described previously under section 7.5 (2). Briefly, HSPC and Chol were determined using Inertsil ODS column (250 x 4.6 mm, 5µ; GL Sciences, Torrance, California, USA), with flow rate of 2.0 ml/min of methanol: water diluent and detected at 12 &16 minutes and 9 minutes respectively using refractive index detector (RID). The content of mPEG-DSPE was determined using a similar method with detection at 6-7 minutes with RID detector and usage of Zorbax C8 stationary phase (150 X 4.6 mm, Agilent, Santa Clara, California, USA) as well as inclusion of ammonium acetate in the mobile phase (2).

8.3.4 Particle size and zeta potential measurements

The particle size, PDI and zeta potential of the optimized liposomal formulations were measured using Zetasizer Nano ZS (0.6 to 6000 nm) with DTS software version 7.11 (Malvern Instruments Ltd., Malvern, UK). The mean hydrodynamic particle diameter was obtained based on the principle of the dynamic light scattering (light source- 633 nm, He-Ne laser; scattering angle- 175°). The samples were appropriately diluted using the external buffer medium while Z-average (in nm) with polydispersity index was reported based on the intensity and volume mode distribution of the particles (intensity-based values have been shown).

The particle size was measured using translational diffusion coefficient by using the Stokes-Einstein equation

$$d(H) = kT/ 3\eta\pi D$$

where d(H) = hydrodynamic diameter; D = translational diffusion coefficient; k = Boltzmann's constant; T = absolute temperature, η = viscosity

Zeta potential (in mV) was measured using electrophoretic disposable zeta cells and values were obtained using the Smoluchowski equation (light source- 633 nm, He-Ne laser; back scattering angle- 175°). All measurements were performed in triplicate (4).

8.3.5 Attenuated total reflection -fourier transform infrared spectroscopy

The prepared drug free liposomes, liposomal VCR, liposomal DOX and Dual drug loaded liposomes (section 8.3.1) were individually spread (200 µl) on the surface of the zinc selenide (ZnSe) ATR crystal while maintaining the lipid concentration at 15 mg/ml for all formulations. The FTIR spectra of individual lipids were obtained after they were dissolved in methanol/chloroform (1:1, v/v), spread on the crystal surface and solvent evaporated under the stream of dry nitrogen gas. The dissolution of the lipids in the solvent mixture and subsequent solvent removal using inert gas ensured the formation of uniform layer of the lipid on the crystal. The spectra for the hydrophilic excipients (ammonium sulphate, l-histidine, sucrose) were prepared by spreading their aqueous solutions individually on the surface of ZnSe crystal. The experiments were carried out using FTIR Microscope & Imaging System (Microscope-Cary 620 FTIR, Spectrometer-Cary 670 FTIR, Agilent Technology Limited, USA). For each sample, a total of 120 scans were collected while having a spectral resolution of 4 cm^{-1}. The obtained data was analysed using Resolutions Pro FTIR Software. The reported spectra were obtained post the baseline correction using blank crystal (4).

8.3.6 Microcalorimetry

The Differential Scanning Calorimetry measurements for the optimized formulations were done using the high-sensitivity Nano-DSC (TA Instruments, USA). The liposomal suspensions and the buffer (external medium of 300 mM sucrose solution pH adjusted to 5.5 using l-lysine) were degassed under vacuum at 23°C for 25 minutes prior to loading in the reference as well as sample cells of the Nano-DSC. The scanning rate was kept at 20°C/ hour with scanning over a temperature range of 20°C to 90°C during the heating and cooling phase with constant pressure at 25 psi for all the samples. All the thermograms were obtained using the same volume of the buffer as reference to prevent erroneous results. The lipid concentration of HSPC as determined by RP-HPLC was found to be 9.58 mg/ml and same was used for the thermodynamic caluclations. Baseline was obtained by repeating the procedure with buffer in

both the cells and then the individual sample thermograms were corrected. The data was analysed using Nanoanalyze software and model fitted using the two-state scaled model to obtain the values of A_w, T_m and ΔH. The samples were analysed in triplicate.

8.3.7 Shape, size, morphology and lamellarity using cryo-TEM

The shape, size, morphology and lamellarity of the liposomal suspensions were evaluated using cryogenic Transmission Electron Microscopy (TECNAI G2 Spirit BioT WIN, FEI-Netherlands) while operating at 200 kV with 0.27 nm resolution. The hydrophobic grid was first converted into hydrophilic by using glow discharge and the samples were spread on grid along with cryo-freezing in liquid nitrogen at -180°C. Post the grid preparation and insertion in cryo-holder, the samples were observed at 70,000X magnification for imaging. For drug free liposomes, vincristine liposomes, doxorubicin liposomes and dual drug liposomes, the bilayer thickness, drug strand width and the distance between the strands was observed using TECNAI software (4, 5).

8.3.8 Morphological evaluation using AFM and FESEM

The surface morphology of the dual drug liposomes was evaluated using the atomic force microscopy (AFM) and Field emission scanning electron microscopy (FESEM).

The AFM of particles was carried out using previously described methods (5). Briefly, the liposomal suspension was taken on a glass slide and vacuum dried while the particle size and surface morphology were analysed using AFM (Agilent 5500, Agilent, Santa Clara, California, USA) with analysis and imaging using software PicoView (Agilent, Agilent, Santa Clara, California, USA).

The external morphological analysis of the optimized dual drug liposomes was done using field emission scanning electron microscopy (FESEM). The FESEM was performed using lyophilized samples of the dual drug loaded liposomes. The formulation (3 ml) was filled in 10 ml clear colourless tubular USP-type I glass vials (Schott, Germany) and half stoppered using 20 mm igloo rubber stopper (Datwyler, Switzerland) and subjected to lyophilization cycle in lyophilizer (SP VirTis Genesis Pilot Lyophilizer, SP Industries, USA). The formulation was

lyophilized using the freezing at -40°C for 8 hours, with subsequent primary drying at -10°C for 72 hours and further secondary drying at +25°C for 24 hours.

The lyophilized samples were spread onto carbon stubs with coating of platinum up to 4 nanometer thickness using ion-spluttering device and observed using FESEM (JEOL, JSM 6100, Tokyo, Japan) (6).

8.3.9 Fixed aqueous layer thickness (FALT) study

The thickness of the aqueous layer around the pegylated liposomes for drug free liposomes, liposomal VCR, liposomal DOX and Dual drug loaded liposomes were evaluated using the previously established methods (2). Briefly the liposomal suspension was ultracentrifuged (OptimaXPN-100, Beckman Coulter, USA) at 60,000 rpm for 4 hours at 4°C for the removal of any unentrapped drug and separation of the supernatant from the pellet. After the removal of the supernatant, the liposomal pellet was resuspended in 300 mM sucrose and added with varying concentrations of sodium chloride (0,10,20,50 mM) with subsequent measurement of the zeta potential as mentioned in section 8.3.4. The thickness of the fixed aqueous layer was calculated as the slope of the zeta potential and Debye-Huckel parameter plot. All measurements were performed in triplicate (7).

8.3.10 Electrolyte-induced flocculation/aggregation

The uniform presence of the pegylation on the surface of the liposomes was evaluated using the electrolyte induced aggregation potential of the optimized formulations (2). Briefly, the liposomal suspension was diluted (1:1) with 10% sodium chloride solution and 10% sucrose solution and incubated at room temperature for 8 hours. The aliquots of the diluted suspensions were withdrawn at 0 hr, 4 hr and 8 hr time points and were evaluated for particle size. All measurements were performed in triplicate.

8.3.11 Interaction with serum proteins and protein adsorption

The interaction potential of the optimized liposomal formulations with the serum proteins was evaluated using the blood from female SD rats (8). Briefly, the blood was collected in eppendorff tubes containing EDTA solution and centrifuged at 3000 rpm for 10 minutes to separate the supernatant blood serum from the sediment of the blood cells. The drug free liposomes, single drug liposomes and dual drug loaded liposomes were added to the blood

serum with incubation for 2 hours at 37±2°C on vibratory shaker at 100 rpm speed. The interaction with serum proteins was evaluated by the measurement of the average hydrodynamic diameter and zeta potential of the optimized liposomal formulations pre- and post-incubation with the blood serum.

The *in-vivo* protein adsorption on the administration of the dual drug liposomes were evaluated by evaluating the *in-vitro* changes in particle size and zeta potential post interaction with albumin protein (9). The dual drug liposomes were mixed with 1% albumin protein solution in 1:1 ratio and incubated for 2 hours at 37±2°C at 100 rpm speed using a vibratory shaker. The drug free liposomes and single drug liposomes were also subjected to the same treatment as a control to evaluate the effects of the carrier components. All measurements were performed in triplicate

8.3.12 Plasma stability study

The in-vitro biological stability of the optimized formulation was evaluated in presence of 50% human plasma by measurement of entrapped drug content and particle size according to methods previously described (10-12). Briefly, commercially available human plasma (Sigma-Aldrich, Bangalore, Karnataka, India) was taken and liposomal suspensions were 100 times diluted with 50% plasma and incubated at 37°C at 150 rpm for 24 hours. The samples were withdrawn at 0,2,4,6,12 and 24 h time points. For determining free drug content in presence of plasma, Superdex 75 was utilized for free drug separation from plasma components and evaluated using aforementioned methods for entrapment efficiency (section 8.3.2). The samples for particle size analysis collected at various time points were ultracentrifuged (OptimaXPN-100, Beckman Coulter, Indianapolis, Indiana USA) at 25000 rpm for 20 mintues at 4°C and collected pellets were washed with Phosphate buffered saline (PBS) thrice before being resuspended in 300 mM sucrose. These samples were then analysed for the hydrodynamic diameter using aforementioned methods (section 8.3.4).

8.3.13 Liposome membrane integrity test

The intactness of the liposomal membrane to retain the drugs on storage was evaluated post active loading of both drugs in the blank liposomes. Briefly, the highly hydrophilic dye 5,6-carboxyfluorescein (CF) at initial concentration of 100 mM was encapsulated inside the blank liposomes at the hydration stage and the liposomal suspension was processed following the

same optimized process as indicated in section 8.3.1. The prepared liposomes were then diluted with fetal bovine serum in 1:5 v/v ratio and incubated at 37°C for 24 hours. The retention (%) of the CF was analysed post suitable dilution in PBS pH 7.4 before and after the membrane disruption using 1% Triton X100. The fluorescence was measured at the excitation emission wavelength of 520 nm/470 nm. Cholesterol free single drug and dual drug loaded liposomes were prepared using the manufacturing process mentioned in section 8.3.1 except for the absence of cholesterol during dissolution of lipids and subsequent ethanolic injection. Drug free liposomes with and without cholesterol were prepared using the method detailed in section 8.3.1. The cholesterol free, normal liposomes (with cholesterol) and empty liposomes were prepared while being evaluated for the latency as control. The percentage latency was determined for the dual drug liposomes, drug free liposomes and cholesterol free dual liposomes at each time point using previously reported equations (13).

8.3.14 Characterization using small angle x-ray scattering (SAXS)

The SAXS intensity profiles of the optimized formulations (empty liposomes, single drug loaded liposomes and dual drug loaded liposomes) were obtained using SAXSpace (AntonPaar, Austria) according to previously described methods (14). The instrument was run using 2.2 kW Sealed tube (line collimation) of X-ray source operating at 40 kV and 50 mA with wavelength of 1.5418 Å. The intensity profiles were collected at 10°C under vacuum for 5 minutes in quartz capillary in triplicate. The collected SAXS data was processed and analysed using PRIMUST software of ATSAS 2.7.2 suite of program available at EMBL-Hamburg website (15). The analysed plots included: Double log plot; Kratky plot; Guinier approximation; pair distance distribution and rigid body modelling.

8.3.15 In-vitro drug release study

The release of the drugs DOX and VCR from the single and dual drug loaded liposomes were evaluated at 37°±0.5 °C in comparison with lipid free drug solutions. Briefly, liposomal suspensions as well as drug solutions containing equivalent amount of Doxorubicin hydrochloride (2 mg/ml) and Vincristine sulphate (1 mg/ml) were placed in 5 ml ready to use dialysis device, Float-A-Lyzer G2 (MWCO: 10kD, Spectrum USA) while being immersed in 250 ml of the release medium phosphate buffered saline pH 7.4, pH 6.4 and acetate buffer pH

5.5 (16). The release medium was kept under stirring at 150 rpm (2 mag systems GmBH, Germany) with samples (1 ml) being withdrawn at pre-determined time points (1,2,4,6, 12 and 24 hours) while the withdrawn volumes were replaced with the fresh release medium. The samples were filtered using 0.22 µm PES syringe filters and evaluated for the content of the two drugs post suitable dilutions using the method described in section 8.3.2.

Additionally, the in-vitro stability in presence of biological fluids was assessed by drug release measurement in presence of bovine serum albumin and 50% human plasma as previously described (12). Briefly, for plasma study, blood from healthy male volunteers (under no drug treatment) was collected in EDTA containing vacutainers and centrifuged (Benchtop, Thermo Fisher Scientific, USA) for 5 minutes at 3000 rpm. The supernatant was separated carefully, liposomal suspensions were 100 times diluted with 50% plasma and incubated at 37°C at 150 rpm for 24 hr. For study of serum-induced drug release, the liposomal suspensions were diluted 10 times with bovine serum albumin (Sigma Aldrich, USA) and incubated at 37°±0.5 °C for 24 hr under stirring at 150 rpm. The samples were withdrawn at previously determined time points. GPC column Superdex 75 (GE healthcare, Singapore) was used for the separation of the released drug from the plasma components and on elution was analyzed using aforementioned methods (section 8.3.2). All the release study experiments were conducted in triplicate and the results were reported as cumulative amount of the drug released at the individual time points.

8.3.16 Drug Release Kinetics

The drug release kinetics for DOX and VCR from the liposomal formulations were obtained by model fitting of the in-vitro drug release data. The evaluated models used included zero-order kinetics, first-order kinetics, Higuchi model, Korsmeyer–Peppas model, and Hixson–Crowell model. Values of regression coefficients (R^2) were determined (6).

8.3.17 Haemolysis Study

To evaluate the haemolysis potential of the formulations to the erythrocytes, the toxicity study was carried out as earlier reported (17). Blood was collected into heparinised tubes post the retroorbital puncture from the rats. This was then centrifuged at 3000 rpm for 5 minutes at 4°C with further reconstitution of the sedimented cell pellet with normal saline to obtain 2% suspension and the process was repeated thrice. A portion of resultant RBC suspension was

then treated with 0.5% v/v solution of Triton X-100 and the absorbance of the haemolyzed cells was measured at 540 nm (taken as 100% values as a positive control for the tested formulations). The absorbance of the RBC suspension at 540 nm on treatment with phosphate buffered saline was taken as the negative control for the tested formulations. The drug solutions and dual drug liposomes were diluted to various concentrations (5000, 500, 50 and 5 µg/ml) with phosphate buffered saline with subsequent incubation with the RBC suspension for 1 hour at 37±2˚C in an incubator. Post incubation, the samples were centrifuged at 3000 rpm for 10 minutes to allow the sedimentation of the non-lysed cell and absorbance of the resultant supernatant was measured after suitable dilution with PBS pH 7.4. The absorbance values of RBC suspension in normal saline were measured and taken as negative control. Additionally, for the doxorubicin containing samples, the absorbance of the doxorubicin at 540 nm in normal saline was measured (to mitigate the absorbance due to chromophore groups present in Doxorubicin) and the values were used for the control of the drug related absorbance. The relative haemolytic potential of each sample was calculated using previously established formula (16).

For formulations without DOX,

$$\% \text{ Haemolysis} = \frac{(A_{540} \text{ of sample} - A_{540} \text{ of negative control})}{(A_{540} \text{ of positive control} - A_{540} \text{ of negative control})} \times 100$$

For formulations with DOX,

$$\% \text{ Haemolysis} = \frac{[A_{540} \text{ of sample} - (A_{540} \text{ of negative control} + A_{540} \text{ of DOX})]}{[A_{540} \text{ of positive control} - (A_{540} \text{ of negative control} + A_{540} \text{ of DOX})]} \times 100$$

Further, to evaluate the effect of the carrier system on RBC, the empty liposomes, single drug loaded liposomes and dual drug loaded liposomes at 5000 µg/ml in normal saline were incubated with the RBC suspension for 1 hour at 37±2˚C. These samples were then observed under the inverted optical microscope Nikon Eclipse TS100 using NIS elements imaging software for the morphological evaluation at 0 hour and 1 hour of incubation.

8.3.18 Stability Study

The stability studies of the single drug loaded as well as the dual drug loaded liposomal suspensions were evaluated on exposure to storage conditions of 2-8°C for 12 months and 25°C/60% RH for 1 month. The reddish orange liposomal suspension was filled (10 ml) in 10 ml clear colourless tubular USP-type I glass vials (Schott, Germany), stoppered using 20 mm bromobutyl rubber stopper (Datwyler, Switzerland) and sealed using 20 mm aluminium flip-off seal (Aditya Pharma, India). The encapsulated drug content, particle size and the zeta potential were evaluated for assessment of stability of drug product. All measurements were performed in triplicate.

8.4 Results and Discussion

8.4.1 Preparation of liposomes

The liposomes under investigation were prepared using the ethanolic injection method. Since both the drugs under evaluation are amphipathic in nature, this method of liposomes manufacture provides the advantage of higher aqueous volume for entrapment as compared to other methods of manufacture (3). This method of liposomes preparation presented various critical process parameters (CPP) and critical material attributes (CMA). Based on the available literature, the critical experimental parameters and critical material attributes were selected and screened by the one-factor-at-time (OFAT) studies. Material attributes such as choice of transmembrane gradient, choice of phosphatidylcholine component, concentration of cholesterol, choice of external medium and choice of the concentration of ammonium sulphate (the transmembrane gradient of choice) were evaluated. Vincristine sulphate has been previously reported for leakage through the lipid bilayer (18). The higher T_m lipid HSPC was taken as the bilayer forming agent while with the concentration of bilayer strengthening agent cholesterol in the range of 38-45% was evaluated to reduce the VCR leakage potential.

8.4.2 Quantification of drugs and lipids in optimised liposomes

The results of the quantification of free drug and entrapped drug are presented in Table 20. The results indicate towards more than 95% of encapsulation of both the drugs with loading efficiencies of 6.06± 0.25% (VCR) and 12.39±1.15% (DOX). Importantly, lyophilization of the dual drug liposomes resulted in slight increase in the free drug content with corresponding

decrease in entrapment efficiency (2-3%) of the liposomal formulation. This negligible change may be attributed to presence of sucrose as cryoprotectant and the hydrophilic drug release from aqueous compartment of the liposomes along with the removal of water during lyophilization (19). The content of the lipids HSPC, Cholesterol and mPEG-DSPE was determined using the RP-HPLC and results indicated towards the presence of more than 95% of all lipids in all the formulated liposomal suspensions (Table 20).

Batch Code	Total lipid (mg/ml)	Assay DOX (%)	FD DOX (%)	EE DOX (%)	LE DOX (%)	Assay VCR (%)	FD VCR (%)	EE VCR (%)	LE VCR (%)	Assay HSPC (%)	Assay Chol (%)	Assay mPEG-DSPE (%)	Particle size (nm)	PDI	Zeta Potential (mV)
B1	15.96	100.35 ±1.49	1.48± 0.25	98.87± 1.88	12.39± 1.15	102.71 ±1.78	5.97± 0.63	96.74± 1.85	6.06± 0.25	98.94± 2.15	97.49± 2.76	99.15± 1.64	95.74± 2.65	0.069	-9.17± 1.19
B2[$]	15.96	-	-	-	-	-	-	-	-	97.48± 3.96	96.37± 2.65	95.38± 2.13	93.32± 3.67	0.083	-24.05 ±1.12
B3[$]	15.96	102.41 ±1.67	2.78± 1.48	99.63± 2.35	12.48± 1.58	-	-	-	-	102.36 ±3.79	98.21± 1.94	100.52± 2.61	98.45± 4.76	0.049	-12.50± 1.25
B4[$]	15.96	-	-	-	-	101.77 ±1.56	4.18± 1.21	97.59± 1.69	6.12± 0.85	100.35 ± 1.78	96.13± 1.69	97.34± 1.16	96.29± 4.41	0.065	-8.00± 1.79
B5[#]	15.96	99.49 ±1.95	2.67± 0.56	96.82± 1.46	12.13± 1.37	100.71 ±2.19	7.16± 0.87	93.55± 2.06	5.86± 0.79	99.69± 2.68	98.35± 1.87	97.63± 1.36	108.56± 3.17	0.096	-8.41± 1.58
B6[@]	15.96	-	-	-	-	99.87	3.18	96.69	6.05	99.15	97.83	98.45	-	-	-

* Abbreviations: DOX= Doxorubicin Hydrochloride; VCR= Vincristine sulphate; FD=Free drug; EE= Entrapment efficiency; LE=Loading efficiency; HSPC= Hydrogenated soy phosphatidylcholine; Chol= Cholesterol; mPEG-DSPE= 1,2-distearoyl-sn-glycero-3-phosphoethanolamine-N-[methoxy(polyethyleneglycol)2000]; PDI= Polydispersity index; [$] B2, B3 and B4 are drug free, DOX liposomes and VCR liposomes respectively, prepared with the composition of the optimized formulation; B5[#] is the lyophilized dual drug liposomes formulation B1; B6[@] FITC loaded VCR liposomal formulation; Results expressed as mean ± SD (n = 3).

Table 20: Results of entrapment efficiency, loading efficiency of DOX and VCR; content of lipids; particle size and zeta potential of optimised formulation.

8.4.3 Particle size and zeta potential measurements

The hydrodynamic diameter and the surface potential of the formulations were evaluated using the quasi-elastic light scattering principle with results being presented in Table 20. All the liposomal formulations exhibited a particle size of around 100 nm with homogenous distribution (PDI values<0.1) while presenting a negative zeta potential. The particle size of dual drug liposome was found to be 95.74± 2.65 nm. The zeta potential of drug free liposomes was found to be -24.05 ±1.12 mV while that of the dual loaded liposomes was -9.17±1.19 mV (Table 20).

8.4.4 Attenuated Total reflection -Fourier transform infrared spectroscopy

ATR-FTIR was used to evaluate the interaction potential of the drugs with the lipids and the formulated liposomes which may lead to physical and chemical instability of the formulations under conditions of storage. The FTIR spectra of the individual drugs, individual lipids, drug free liposomes, single drug loaded liposomes and dual drug liposomes were obtained and evaluated for the presence of such interactions. The spectra of the individual drugs, lipids and other excipients are presented in Figure 35 while that of the drug free liposomes, DOX liposomes, VCR liposomes and dual drug liposomes are presented in Figure 36. Doxorubicin FTIR spectrum (Figure 35 a) displays characteristic bands below 1500 cm^{-1} at 1260–1000 cm^{-1} (carbonyl CO stretching of alcohol) and 900–675 cm^{-1} (out of plane OH bending). However, spectrum of DOX liposomes does not display these characteristic peaks indicating towards the encapsulation of the drug inside the liposomes and probably not in the lipid bilayer. Similarly, the spectrum of VCR liposomes does not exhibit the characteristic FTIR bands of VCR (figure 35 h) at 3393cm^{-1} (OH group), at 2360 cm^{-1} (stretching vibration of C-H bond), at 1458 cm^{-1} (presence of C=C group) and absorption bands due to asymmetric and symmetric modes of O-C-O bond at 1098cm^{-1} and 1048 cm^{-1} respectively. Additionally, the characteristic stretching vibration frequencies (at 3300cm^{-1}, 2900cm^{-1} and 1600 cm^{-1}) observed in the drugs due to presence of functional groups such as NH_2, CO, OH are not observed in any of the drug loaded liposomal formulations which further points towards the presence of the drugs inside in the liposomal formulations with lack of interaction with the lipids as well as the formed liposomal bilayer. Further, all the formulated liposomes exhibited bands at 2958 cm^{-1} (asymmetric CH_3

stretching), 2925 cm^{-1}(asymmetric CH_2 stretching), 2853 cm^{-1} (symmetric CH_2 stretching), 1735 cm^{-1}(C=O stretch), 1472 cm^{-1} (CH_2 acyl scissoring), 1375 cm^{-1} (CH_3 bend), 1252 cm^{-1} (asymmetric P=O stretch), 1173 cm^{-1}(O-C-O stretch), 1093 cm^{-1}(symmetric P=O stretch), 1019 cm^{-1}(C-OP stretch) and 970 cm^{-1}(asymmetric C-N^+-C stretch) characteristic to the bilayer forming lipid HSPC (Figure 35 f, 36). Similarly, the secondary C-OH band characteristic of cholesterol (at 1049 cm^{-1}) (figure 35 e) and CH alkyl stretching (2922 cm^{-1} and 2848 cm^{-1}) as well as C=O stretch (1738 cm^{-1}) of mpeg-2k-DSPE (figure 35 g) was observed in all the liposomal formulations (Figure 35, 36). These results indicate towards the formation of the bilayer for all formulations using HSPC, cholesterol and mpeg-2k-DSPE with lack of any interactions with the drugs when incorporated separately or together. Further, the absence of any drug associated peaks in all drug loaded formulations as compared to drug free liposomes indicate the encapsulation of the drug inside the liposomal core and their absence in the lipid bilayer (20). However, since both the drugs are amphiphilic in nature with published reports suggesting towards their preferential incorporation in the liposomal aqueous core, evaluation of the drug-drug interaction in case of dual drug loaded liposomes needs to ascertained using an orthogonal technique like microcalorimetry (21).

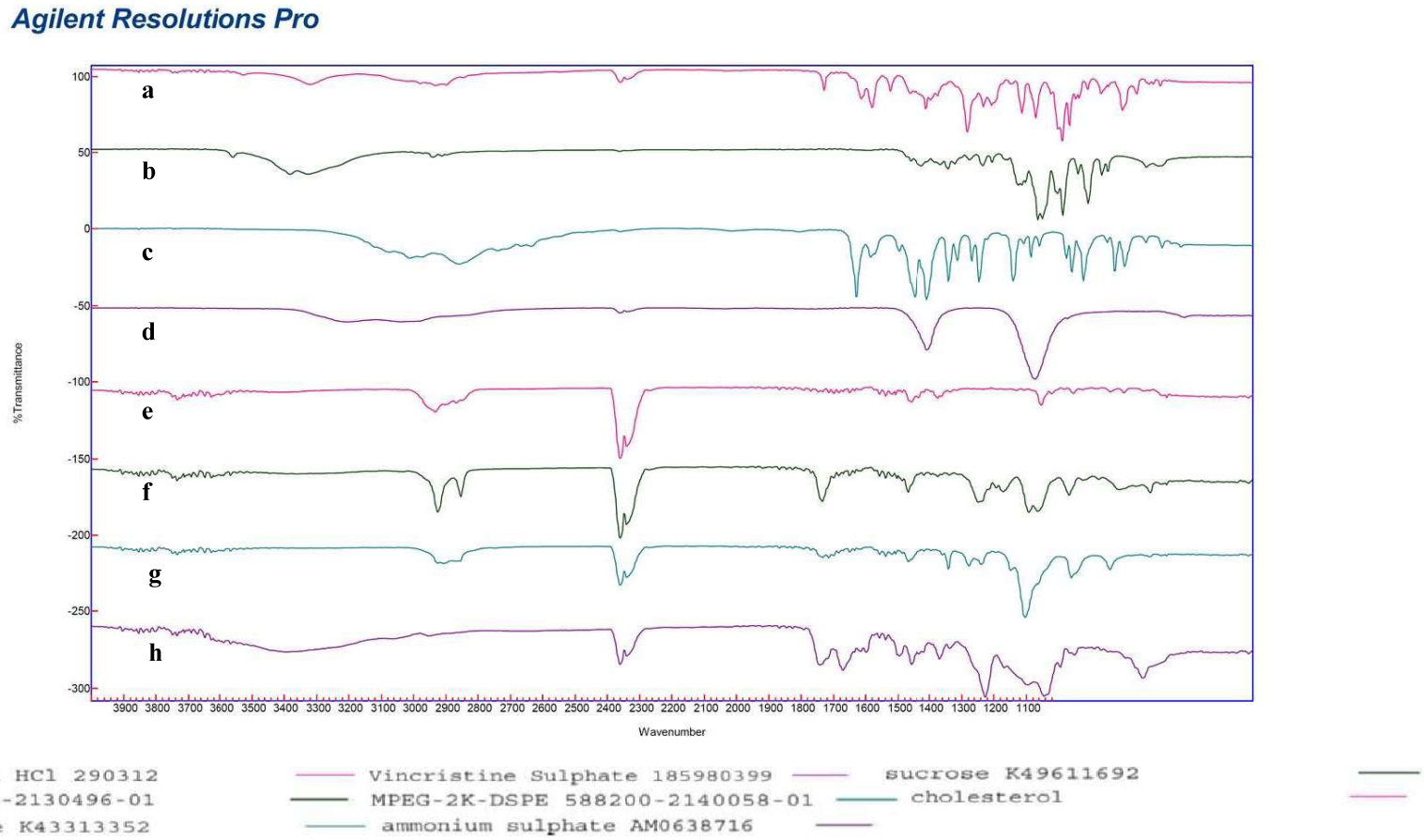

Figure 35: Attenuated total reflection-Fourier transform infrared spectroscopy spectrum for Doxorubicin (a), l-Histidine (b), Sucrose (c), Ammonium sulphate (d), Cholesterol (e), HSPC (f), mpeg-2000-DSPE (g) and Vincristine (h).

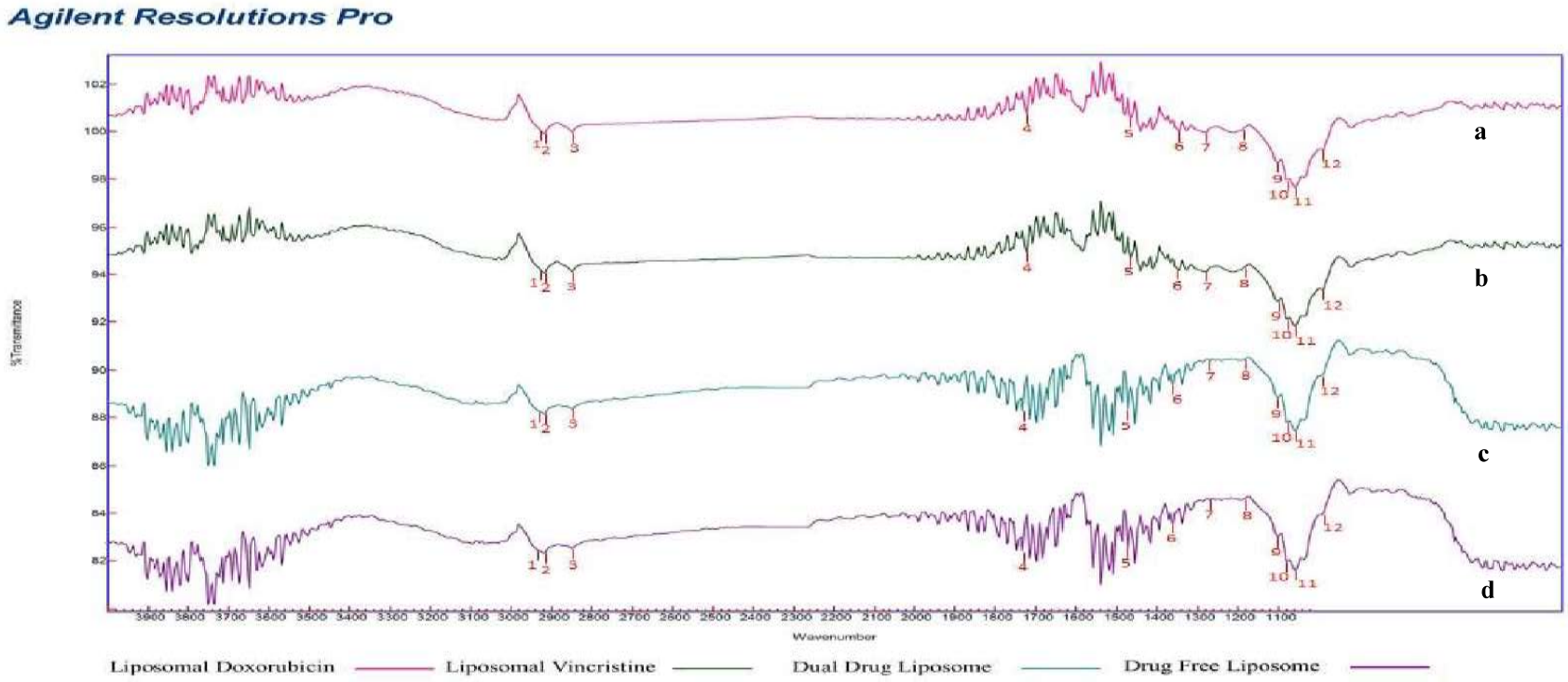

Figure 36: Attenuated total reflection-Fourier transform infrared spectroscopy spectrum for DOX liposomes (a), VCR liposomes (b), dual drug liposomes (c) and drug-free liposomes (d) with labelled peaks (P) of HSPC (P1: 2958/cm; P3: 2853/cm; P5:1472/cm; P6:1375/cm; P7: 1252/cm; P8: 1173/cm; P9: 1093/cm; P11: 1019/cm; P12: 970/cm); cholesterol (P2: 2922/cm; P10: 1049/cm) and mPEG-2k-DSPE (P4: 1738/cm).

8.4.5 Microcalorimetry

The evaluation of the thermotropic behaviour of the optimized liposomal formulations (drug free, DOX Liposomes, VCR liposomes, dual drug liposomes) as well as the interaction potential of the drugs with the lipid bilayer was evaluated using the highly sensitive "Nano-DSC) microcalorimetry. The liposomes are made of bilayer forming lipid blocks of HSPC, Cholesterol and mpeg-DSPE with each of them presenting characteristic phase transition temperatures alternating between the closely packed ordered gel phase and disordered loosely oriented crystalline phase. In this experiment, energy was added to the liposomal formulations in suspension form to evaluate the thermal transition (change in enthalpy) behaviour while heating between 10°C to 90°C and then cooling back to the starting temperature. The triplicate scans were found to be superimposable with the thermograms during the cooling phase exhibiting retracing that of the heating phase indicating the absence of degradation (4).

The experimental thermograms indicate towards the presence of characteristic endothermic broad peak of the phospholipid HSPC at 51.57±3.28°C in all the formulations which represented its phase transition temperature (T_m~55°C) in the formulated liposomes (Figure 37 A-D) (22). Interestingly, the endothermic peak was observed despite having a high concentration (~38%) of the bilayer rigidifying lipid cholesterol. Another endotherm was observed at 68.75±1.07°C in the DOX loaded and dual drug loaded liposomes while it was absent in the drug free and the VCR liposomes. This may be attributed to the thermal melting of the formed doxorubicin sulphate crystals present in the aqueous compartment as reported earlier in the literature (23). Further, the enthalpy change was found to have a similar pattern as observed in Doxil™ and Lipodox™ thereby indicating the similarity in physico-chemical properties of the earlier with the later (23). The observed first endotherm is similar in both the DOX containing liposomes (Figure 37 C and 37 D) as compared to drug free liposomes (Figure 37 A) which indicates towards the absence of drug interactions with the lipid bilayer. However, a slight change was observed in the membrane transition endotherm of VCR liposomes (Figure 37 B) as compared to the drug free liposomes (Figure 37 A) which may be attributed to the interaction potential of the VCR with the inner mpeg-DSPE layer previously reported in literature (24). Importantly, the same change was not observed in case of dual loaded liposomes (Figure 37 D). The endothermic peaks were found to be reversible in nature (during heating-

cooling phase) indicating towards the physico-chemical stability of the formulations on exposure to transient elevated temperatures as well as the non-leaky nature of the formed lipid bilayer

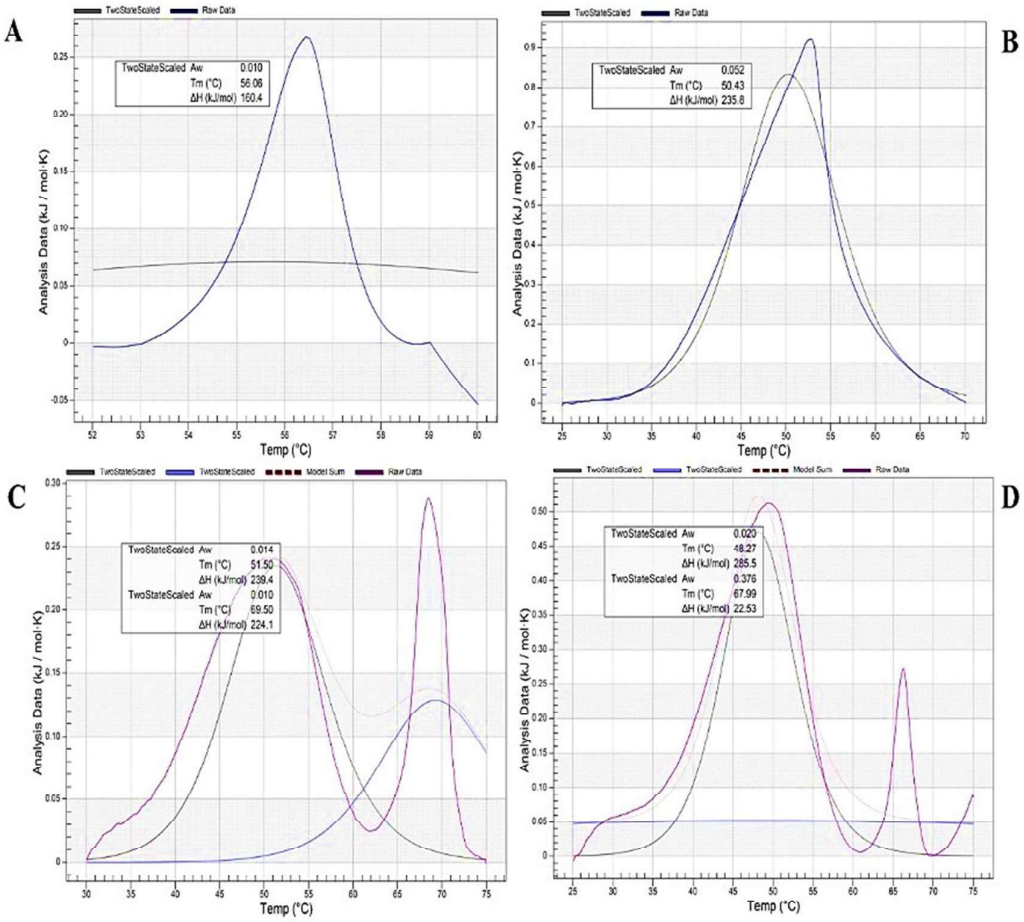

Figure 37: Microcalorimetry- Differential scanning calorimetry of drug free liposomes (A), VCR liposomes (B); DOX liposomes (C) and dual drug liposomes (D)

8.4.6 Shape, size, morphology and lamellarity using cryo-TEM

Cryogenic transmission electron microscopy (cryo-TEM) was used for the assessment of the shape, size, morphology and lamellarity of the optimized liposomal formulations. This

approach allows the study of the samples in native state at the cryogenic temperatures removing the need of additionally processing conditions. The results of the cryo-TEM imaging are represented in Figure 38 and Table 21. The size distribution patterns of all formulations were in accordance with that determined by DLS with values of less than 100 nm. The drug free liposomes, single loaded liposomes and dual drug liposomes exhibited spherical unilamellar structures with similar bilayer thickness. The interior of DOX loaded single drug and dual drug liposomes showed the characteristic doxorubicin sulphate nanorod crystals in "coffee-bean shaped" structures while the interior of VCR loaded liposomes exhibits electron dense VCR-sulphate precipitation as compared with drug free liposomes (25). The nanoprecipitation of DOX with ammonium sulphate in the internal aqueous compartment results in the formation of nanorods or strands (characterized by the strand size and inter-strand space). The internal morphology of dual drug liposomes looks similar to overlay of DOX liposomes and VCR liposomes as well as the ones observed in commercially available liposomal doxorubicin (2). Additionally, the unilamellar nature of optimized liposomal formulations indicate towards absence of additional drug presence and carrier mediated changes in drug release (25). Similarity of the TEM images, particle size and morphology of the optimized liposomal suspensions to the clinically used formulation indicate towards improved chances of passive uptake by the tumor cells (26).

Product	Average Size (nm)	Bilayer thickness (nm)	Strand size (nm)	Inter-strand distance (nm)	Lamellarity
Drug free liposomes	68.87	3.98	-	-	Unilameller
VCR Liposomes	71.42	4.01	-	-	Unilameller
DOX Liposomes	76.77	4.02	17.83	2.02	Unilameller
DOX+VCR Liposomes	78.93	4.05	18.05	1.97	Unilameller

Table 21: Results of characterization using cryo-Transmission electron microscopic (TEM) analysis of the pictographs.

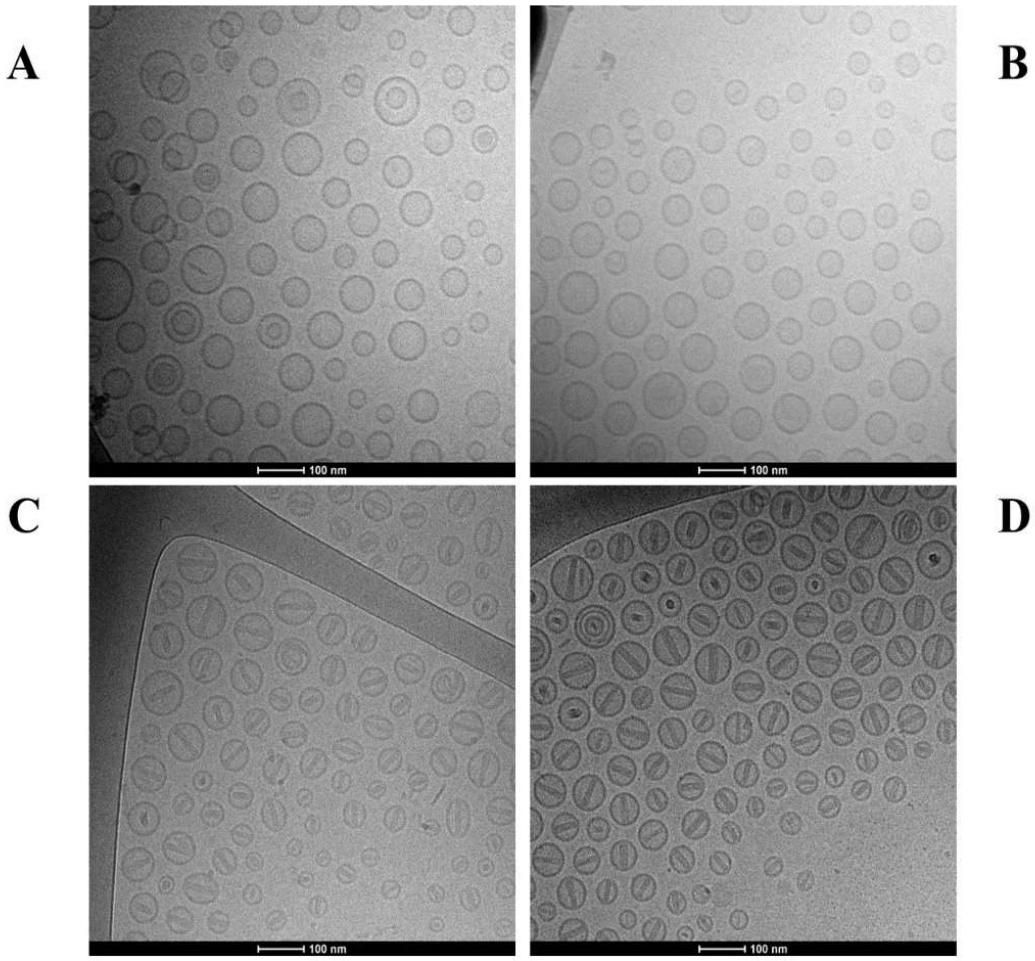

Figure 38: Cryogenic Transmission electron microscopy of drug free liposomes (A), VCR liposomes (B); DOX liposomes (C) and dual drug liposomes (D)

8.4.7 Morphological evaluation using AFM and FESEM

The morphological evaluation of the optimized dual drug loaded liposomal formulation was further done using AFM (Figure 39) and FESEM (Figure 40). The AFM image (Figure 39 A) and 3D construction (Figure 39 B) indicates towards the spherical nature of the particles with size of 97.4 nm. The FESEM results (Figure 40) further confirm the spherical external morphology of the particles with a size of around 100 nm.

Morphological evaluation of the liposomal formulation was done using AFM, FESEM and cryo-TEM to evaluate the effect of the additional drug loading into the liposomal DOX. The

results indicate towards spherical external surface of the liposomes having a hydrodynamic diameter of 100 nm while presenting the characteristic internal DOX sulphate nanocrystals. These data are in good correlation with the results of the hydrodynamic diameter from DLS experiments and are suggestive of the enhanced passive permeation into tumor cells similar to that of liposomal doxorubicin.

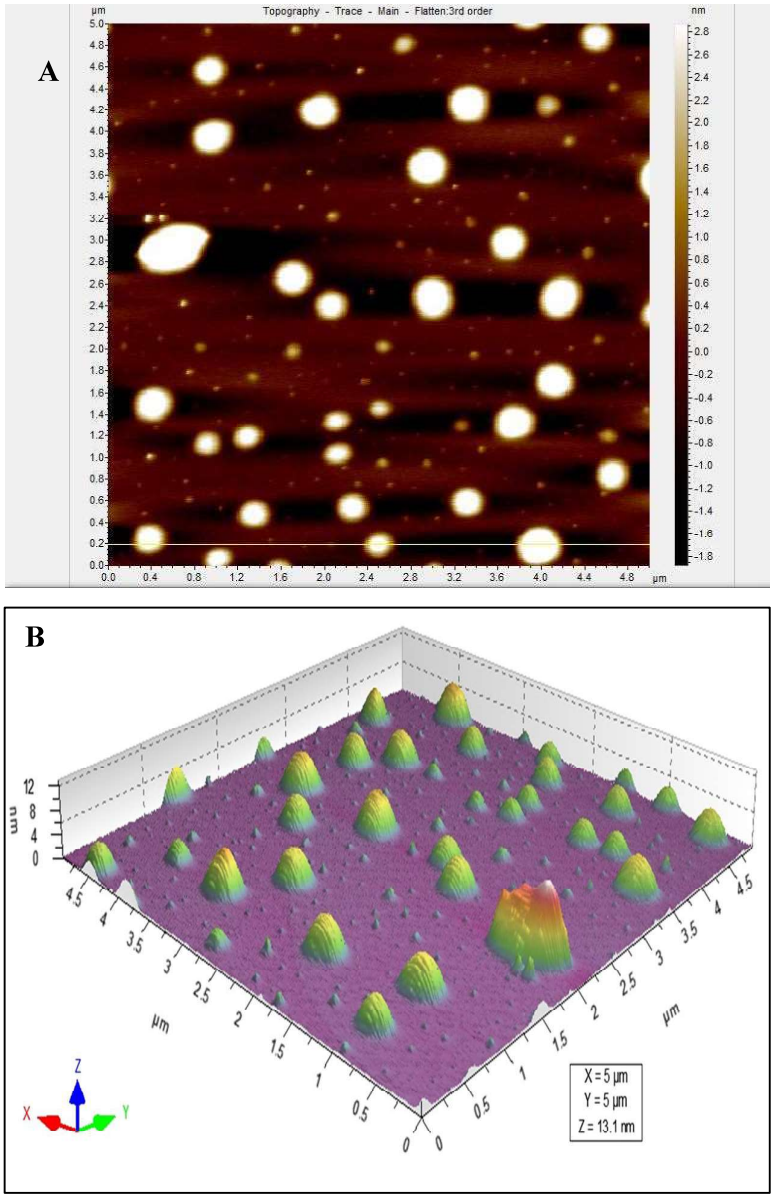

Figure 39: Evaluation of morphology of the dual drug liposomes using AFM (A) and its 3D reconstruction (B)

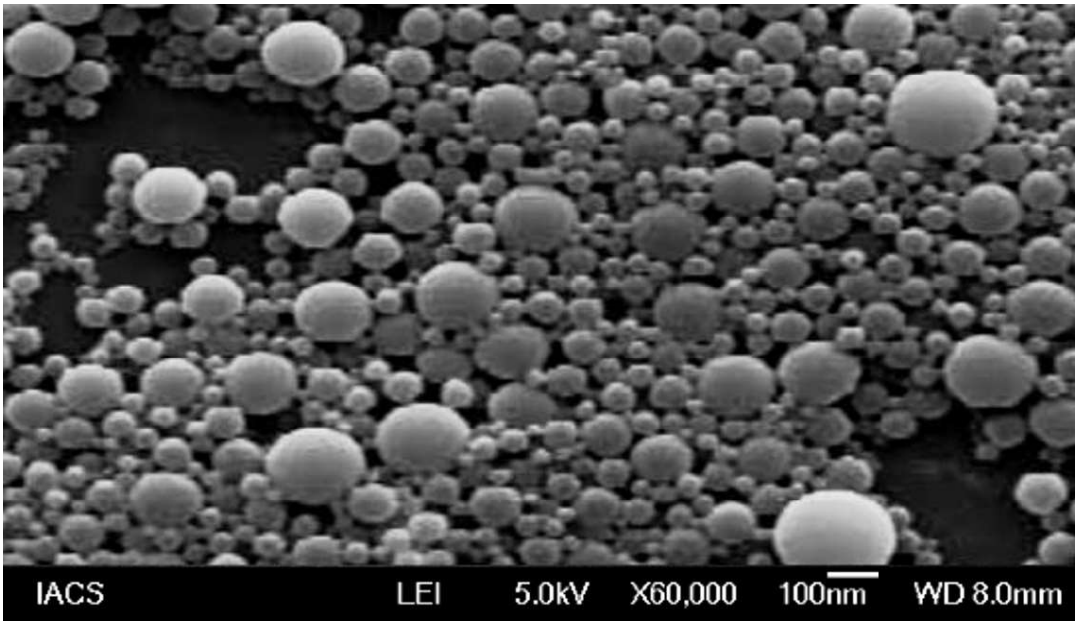

Figure 40: Evaluation of morphology of the dual drug liposomes using FESEM

8.4.8 Fixed aqueous layer thickness (FALT) study

FALT study was used to measure the grafted PEG layer thickness /fixed aqueous layer associated with the optimized liposomal formulation which may functionally prevent the interactions with the serum proteins ensuring the long circulation potential of the formulated nanoconstructs. Presence of surface pegylation has been reported to provide strong steric hindrance against such interactions with serum components (2). This position of the slipping plane was measured from the electrolyte-based changes in the zeta potential of the liposomes and is presented in Table 22. The aqueous layer thickness was found to have increased in the drug loaded liposomes as compared to the drug free liposomes with dual drug loaded liposomes exhibiting the highest value of fixed aqueous layer among all liposomes. The difference in the observed results between the liposomal formulations may be attributed to the encapsulated drug (DOX, VCR, DOX+VCR) mediated alteration of the lipid membrane associated physiochemical parameters like zeta potential. The slightly higher FALT values of Dual drug liposomes than the clinically tested Liposomal Doxorubicin hydrochloride indicated towards possible long circulation nature of the formulated therapeutic carrier. These results are in good co-relation with the previously reported results (2).

8.4.9 Electrolyte-induced flocculation/aggregation

The uniformity and stability of the pegylation chains on surface of the liposomes was evaluated using electrolyte induced aggregation study. The incubation of the optimized drug free and drug encapsulated liposomes with electrolytes over 8 hours showed no increase in the hydrodynamic diameter of the liposomes (Table 22). The presence of stable uniform pegylation chain provides steric hindrance to interaction with the elements of reticuloendothelial system (RES) along with the prevention of aggregation. These results indicate towards the presence of uniform pegylation layer on the surface of the optimized liposomal formulation. The results of FALT and the electrolyte induced aggregation shows a non-significant difference from the marketed liposomal formulation and indicate towards the prevention of opsonisation as well as long blood circulation time (27, 28).

8.4.10 Interaction with Serum proteins and protein adsorption

The optimized dual drug formulation was evaluated for the stability in serum proteins as well as interaction potential with human serum albumin by measurement of the changes in particle size and the zeta potential. This evaluation serves to assess the in-vivo stability of the formulations in serum on circulation. Importantly, serum proteins have been reported to have potential adsorption properties on hydrophobic surfaces of liposomal surface components resulting in the increased conformational entropy and subsequently the increased chances of opsonisation by the components of MPC as well as accelerated blood clearance. Consequently, such interactions will lead to loss of liposomal membrane integrity, the release of active components at unintended sites, loss in efficacy of the tested formulations as well as increased toxicity profile (29, 30). The size as well as charge parameters were evaluated for the dual drug liposomes in native state (control for the exposed conditions) and post incubation (2 hours) with serum as well as albumin (Table 23). The values of surface potential and particle size in case of liposomal samples exposed to serum as well as albumin exhibit non-significant difference with the results of control sample. Further, the values of the polydispersity index indicate towards the homogenous size distribution of the particles even on exposure with the serum components. These results indicate towards the stability of the drug carrier in the serum

and in presence of albumin, thereby maintaining the integrity of the carrier during transit as well as reducing the probability of the drug release and associated toxicity. These results along with those of the electrolyte induced aggregation confirm the presence of uniform pegylation layer as well as absence of the serum protein induced instability of the formulated liposomal suspension thereby confirming the suitability of systemic delivery of such carrier system to deliver the drugs to the intended sites. Additionally, these stability results may be attributed to the use of bilayer forming phospholipids having phase transition temperature higher than 37°C and the surface decoration using mpeg-DSPE (31).

Formulation	FALT (nm)	Electrolyte induced aggregation study		
		Particle Size (nm) _0 hour (PDI)	Particle Size (nm) _4 hour (PDI)	Particle Size (nm) _8 hour (PDI)
Drug free liposomes	2.927 ±0.042	86.47± 1.78 (0.121)	85.23± 1.54 (0.071)	87.18± 1.21 (0.113)
DOX Liposomes	3.334±0.058	106.4± 1.41 (0.117)	105.5± 1.71 (0.067)	105.3± 1.78 (0.078)
VCR Liposomes	3.567±0.039	106.2± 1.15 (0.083)	108.7± 1.82 (0.076)	105.5± 2.18 (0.074)
DOX+VCR Liposomes	3.764±0.026	107.6± 1.02 (0.112)	107.7± 1.15 (0.035)	109.1± 1.53 (0.105)

Table 22: Results of fixed aqueous layer thickness (FALT) and electrolyte induced aggregation (EIG) study. Results of the FALT and EIG study are presented as mean ± SD (n=3).

Formulation	Native Liposomal suspension			After incubation with Serum			Protein stability		
	Initial			After 2 hours			After 2 hours		
	Z. Potential (mV)	P size (in nm)	PDI	Z. Potential (mV)	P size (in nm)	PDI	Z. Potential (mV)	P size (in nm)	PDI
Drug free liposomes	-24.05±4.45	93.32±2.31	0.083	-26.31±1.17	95.04±3.15	0.068	-25.51±3.45	92.41±2.91	0.101
DOX Liposomes	-14.50±2.57	108.3±1.31	0.134	-16.06±1.39	106.2±2.18	0.108	-15.50±3.59	107.2±1.52	0.056
VCR Liposomes	-8.00±1.89	113.2 ± 1.58	0.086	-9.41±2.15	111.9±2.13	0.074	-8.65±2.66	112.6±1.67	0.094
DOX+VCR Liposomes	-5.76±3.15	115.2 ± 1.14	0.057	-6.58±1.85	116.8±1.51	0.088	-6.21±1.29	114.7±2.45	0.073

Table 23: Results of zeta potential and hydrodynamic diameter before and after incubation with the serum and proteins. Results of the study are presented as mean ± SD (n=3).

8.4.11 Plasma stability study

The results of entrapped drug content and particle size profile of optimised liposomes in presence of human plasma stability is presented in Table 24. The results show a cumulative release of 14% DOX and 25% VCR over the study period. Additionally, an increase in particle size of the formulations was observed (after 2 hours) on incubation with plasma over 24 hours. The plasma drug release profile indicated slower release of DOX as compared to VCR which may be attributed to DOX release from insoluble DOX sulphate nanocrystals while VCR is released from soluble VCR sulphate. The increase in particle size after 2 hours may be attributed to presence of biomolecular protein corona. These results of dual drug liposomes show non-significant difference from single drug liposomes and are in good correlation with previously reported studies (2, 10). These results indicate that dual drug liposomes on intravenous administration are stable for atleast 24 hours.

Time (hr)	Entrapped Drug content (%)				Particle size (nm) (PDI)		
	DOX-L	VCR-L	Dual L-DOX	Dual L-VCR	DOX-L	VCR-L	Dual L
0	97.22± 0.81	95.85± 1.18	98.52± 0.95	94.03± 1.08	98.45± 4.76 (0.049)	96.29±4.41 (0.065)	95.74±2.65 (0.069)
2	96.55± 0.81	95.85± 1.18	98.52± 0.95	94.03± 1.08	104.78± 3.21 (0.082) *	103.32±2.69 (0.096) *	100.25±1.81 (0.090) *
4	94.41± 1.16	89.38± 1.33	95.39± 1.19	90.32± 1.56	106.34± 2.95 (0.093) *#	104.87±3.05 (0.096) *#	101.25±2.36 (0.076) *#
6	92.27± 1.35	85.24 ± 1.51	93.41± 0.87	86.45± 0.94	105.59± 3.71 (0.108) *#	106.79±2.86 (0.119) *#	102.43±1.61 (0.063) *#
12	89.75± 0.98	83.23± 2.13	90.12± 1.38	84.09± 1.68	106.88± 4.39 (0.091) *#	106.53±3.78 (0.105) *#	103.71±3.51 (0.088) *#
24	85.64± 1.43	73.32± 2.66	87.48± 1.29	75.24± 2.49	108.31± 2.88 (0.074) *#	108.89±3.19 (0.113) *#	104.55±3.84 (0.109) *#

Results expressed as mean ± SD (n = 3); DOX-L: liposomal doxorubicin, VCR-L: liposomal Vincristine, Dual L: Dual drug liposomes; * indicates significant ($p<0.05$) difference in particle size with 0-hour values of each formulation; * indicates non-significant ($p>0.05$) difference in particle size with 2-hour values of each formulation

Table 24: Plasma stability profile of optimized formulations- entrapped drug and particle size over 24 hours.

8.4.12 Liposome membrane integrity test

To study the effect of cholesterol in the composition and to determine whether dual loading in the liposomes has any significant impact on the lipid structures integrity, that may occur in the presence of serum components, carboxy-fluorescein (CF) leakage assay was performed. CF was incorporated during the hydration stage at high concentration (100 mM) and its latency was measured from the liposomal formulations after incubation with serum at different time points. We observed that in all the formulations prepared without cholesterol in it, the %CF retention was between 45-55% at initial stage whereas that for optimized liposomal formulations it was between 88-95% (Figure 41). This suggests that cholesterol has significant effect on integrity of the bilayer and imparts rigidity to the layers, prevents leakage of drug and affects phase transition at the levels selected. Release study for 24 hr suggests, that the optimized dual loaded liposomal composition without cholesterol showed the release of encapsulated CF gradually to a final level of around 30% while that with cholesterol showed retention of approx. 85% of CF. At the end of 24 hr, only a marginal release from the cholesterol containing liposomes as compared to initial levels was observed, suggesting the dual loading has not significantly led to any membrane perturbations and will remain intact during the circulation while in contact with various serum proteins.

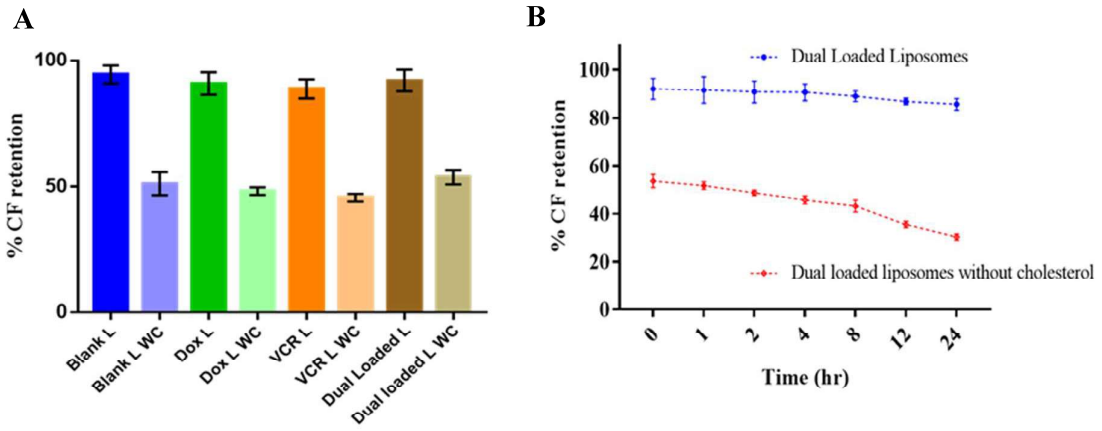

Figure 41: (A) %CF retention in various formulations (B) Percentage carboxy-fluorescein (CF) retention at different time points for dual loaded liposomes with and without cholesterol (L: Liposomes; WC: Without Cholesterol).

8.3.13 Characterization using small angle x-ray scattering (SAXS)

Small angle X-ray scattering (SAXS) has been widely used as an advanced characterization tool to provide useful insights into the structural parameters of liposomes while being present in the native state and offered a powerful complimentary tool to the already established analytical techniques (32). Typically, SAXS measurements of nanosized structures represented intensity of scattering of incident X-rays as a function of scattering angle and may be used to determine the particle size, morphology, aggregation potential, degree of disorderliness, as well as effect of drug loading into liposomes among others. The SAXS measurement profile of the blank liposomes, single drug liposomes and dual drug liposomes were presented in Figure 42 with the ATSAS processed parameters being presented in table 25. The double log plots (log intensity vs log momentum transfer q) were prepared for estimation of liposomal component real vector and level of aggregation of the liposomal suspensions (Figure 42A). The results indicated the presence of scattering component in real space at 9.1 nm^{-1} in blank liposomes with a shift to 9.4 nm^{-1} for the drug loaded liposomes and a real vector peak at 0.67-0.69 nm^{-1}. The shift in the real vector in the drug loaded liposomes as compared to drug free liposomes indicated the drug loading in the liposomes while similarity in the value of the real vector of drug loaded liposomes indicated the incorporation of drugs in the same compartment of liposomes. Since, no sharp increase was observed in the scattering intensity of the tested liposomal formulations, the results showed the lack of aggregation potential of the samples which were in good correlation with the results of electrolyte induced aggregation study. The slope of Guinier plot approximation (ln I(q) vs q^2) presented the radius of gyration (R_g) related to the size of the particle and the shape of the particle) while the ordinate value exhibited the maximum dimension D_{max} (distance distribution approximating to zero) which indicated particle size of the nanoliposomes (Table 25). The scattering intensity profile showed single ellipsoidal structure of all the drug loaded liposomes while the drug free liposomes presented hollow structure particles. The results of R_g and Dmax presented the similarity in size parameters of the formulated carriers, morphology and D_{max} results which were in good correlation with those obtained from TEM. These results may be attributed to the drug loading into the aqueous layer component of liposomes resulting in similarity of the parameters derived from Guinier approximation (33). Further, the pair distribution profile of liposomal formulations (Figure 42B) provided additional confirmation of the results. The Kratky plots

(I(q)*q^2 vs q): Figure 42C) indicated high level of orderliness (stable globular systems indicated by peak profile) in all liposomal formulations except the VCR liposomes (unstable indicated by rising hyperbola profile). This lack of orderliness in case of the VCR liposomes may be attributed to the free drug which may be present in the solution due to its leakage potential from the formulation. The particle volume (correlated to particle molecular mass) obtained from the Porod-Debye plot (I*q^4 vs q: integral of Kratky Curve-Figure 42D) showed the increase in volume for the drug loading formulations (dual drug loaded particles present the highest volume). These difference in calculated volume may be attributed to increased scattering intensity from the doxorubicin sulphate nanocrystals as compared to the VCR solution present inside the liposomes, resulting in higher values in the DOX loaded liposomes. Additionally, the presence of the VCR in addition to DOX crystals in the dual liposomes resulted in higher volume as compared to the other tested formulations. The rising hyperbola observed in the plot of all the formulations indicated the absence of aggregation and similarity in the physicochemical nature of all formulated liposomes (34). These results were then used for the uniform density rigid body modelling (Figure 42 E-H presented as non-bonded spheres with three orthogonal views) which presented the structural characteristics best fitted to the available data. The results exhibited the presence of dense components towards the central core of the structures in DOX and dual drug loaded liposomes as compared to the drug free liposomes while similar scattering intensity molecules at the centre and the edges were observed for VCR liposomes. The dual drug liposomes model indicated the superimposition of both DOX liposomes and VCR liposomes models without the presence of any observed components towards the edges. This indicated the presence of DOX and VCR in predominantly inside the liposomes in dual liposomes as well as DOX liposomes whereas the presence of VCR outside the liposomes in addition to the presence in the core (VCR liposomes) (35). Importantly the results of the SAXS analysis of the liposomal formulations were in good correlation with the results obtained from the other orthogonal techniques and indicated the intrinsic stability of the formulations and the presence of necessary physicochemical characteristics suitable for delivery of the drugs (36).

Product	Paired Distribution		Particle volume	Structural Morphology
	Dimension D_{max} (nm)	Radius of Gyration (nm)		
Drug free liposomes	48	15.1	3.62	Hollow particle
VCR Liposomes	50	15.6	4.87	Single lobe ellipsoid
DOX Liposomes	52	15.4	5.27	Single lobe ellipsoid
DOX+VCR Liposomes	55	15.4	5.38	Single lobe ellipsoid

Table 25: Results of characterization using small angle X-ray scattering (SAXS) for drug free liposomes, VCR liposomes; DOX liposomes and dual drug liposomes.

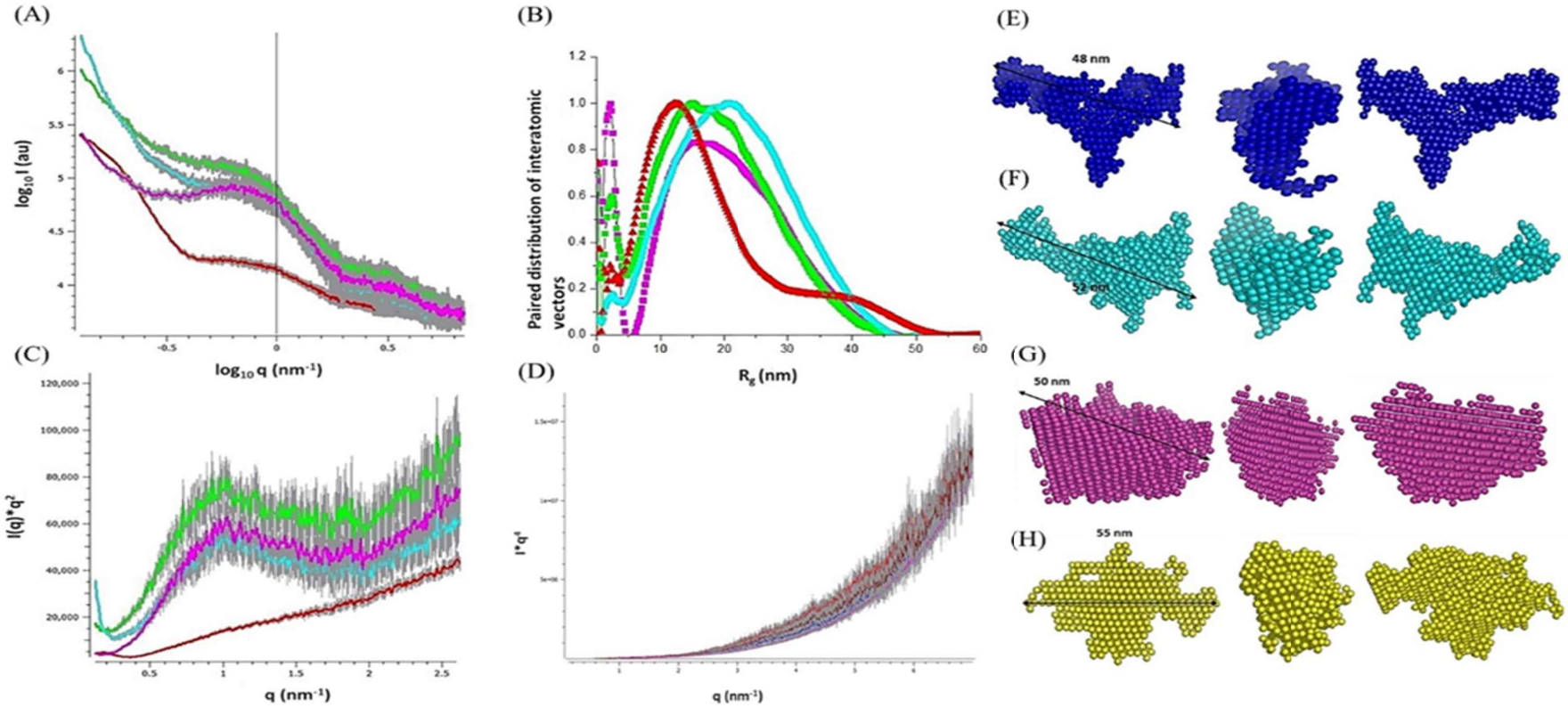

Figure 42: Characterization plots using Small Angle X-ray scattering: A) Double log plot B) paired distribution profile C) Kratky plot D) Porod-Debye Plot. The uniform density models of drug free liposomes (E), DOX liposomes (F), VCR liposomes (G) and Dual drug liposomes (H). The colour coding for each plot: dual drug liposomes- green (A, B, C), red (D); drug free liposomes- red (A, B), cyan (C), brown (D); VCR liposomes- cyan (A, B), red (C), blue (D); DOX liposomes- magenta (A, B, C, D).

8.3.14 In-vitro drug release study

The assessment of the DOX and VCR release from the formulated liposomes under the conditions which these carriers may encounter in normal tissues, cancerous tissues and inside the cancerous cells was evaluated by the in-vitro drug release profiling from the optimized formulations at various pH (7.4, 6.4, 5.5) at 37 ˚C for 24 hours. The results of drug release from the formulations and the carrier free drug solutions are presented in figure 43 A-C. Release of both drugs from carrier free drug solution were observed more than 85% at all the three pH after 4 hr and a complete release (100%) was observed by 6 hrs. The release from carrier free drug solution was evaluated as a control to ensure the intrinsic stability of the drugs in solution at the tested pH conditions over the entire duration of the study as well as the permeability of these low molecular weight substances through the dialysis devices used in the study. The DOX release from single drug liposomes showed pH associated increased release with cumulative values at the end of 24 hrs being around 36%, 42% and 54% respectively at pH 7.4, 6.4 and 5.5. Similar release profile was observed in case of dual loaded liposomes with corresponding cumulative drug release of 31%, 37% and 51% at the three tested pH conditions. These results indicated the slow-release profile of DOX from DOX sulphate nanocrystals ($t_{50\%}$ of 24 hours for both DOX liposomes) with release being a function of pH dependent stability of the precipitate in both DOX liposomal formulations. The results indicated that the formulations may present higher drug release inside the tumor cells as compared to the normal tissues and are similar to the earlier reported drug release profiles (37).

Interestingly, although VCR loaded liposomes had same composition as compared to DOX liposomes, the VCR release from both the single and dual loaded formulations exhibited an initial burst release of 20% irrespective of the pH conditions with $t_{50\%}$ of 4-6 hours along with a $t_{90\%}$ of 24 hours. The results of faster VCR release may be attributed to presence of VCR sulphate in solubilized form inside the liposomal formulations and exhibiting increased permeability through the liposomal bilayer under the different pH conditions. These experimental VCR release profiles were found to be similar to that of earlier reported liposomal VCR release profiles (38). Importantly, the DOX and VCR release from the dual drug liposomes showed similar profiles as compared to that from the single loaded liposomes indicating towards the lack of alteration of the individual release patterns due to the presence

of second drug in the formulation. Such similar drug release profiles of dual drug liposomes as compared to single liposomes presenting unaltered drug release of the individual drugs without alteration due to presence of another active component may invariably help in achievement of therapeutically effective co-spatial presence of both the drugs at the tumor site (39).

The DOX and VCR release from the formulated liposomal formulations on dilution with biological fluids was evaluated for assessment of dilution-induced drug release. Interaction with the plasma resulted in the release of the free DOX and VCR from the liposomal formulations at 0 hour (Figure 43 D). While VCR containing formulations exhibited approximately 25% drug release over 24 hours, DOX containing formulations showed non-significant (<5%) increase in the drug release. Additionally, interaction with serum albumin resulted in drug release of 15% and 40% of DOX and VCR respectively from all liposomal presentations after 24 hours (Figure 43 E).

These results indicated the stability of dual drug loaded nanoliposomal suspension post intravenous injection and during plasma circulation as well as transit from the injection site to the target organ. The characteristics of drug release presented by the dual drug nanoliposomes at varying pH conditions and in presence of biological fluids were found to be similar to that of the clinically used liposomal doxorubicin (2).

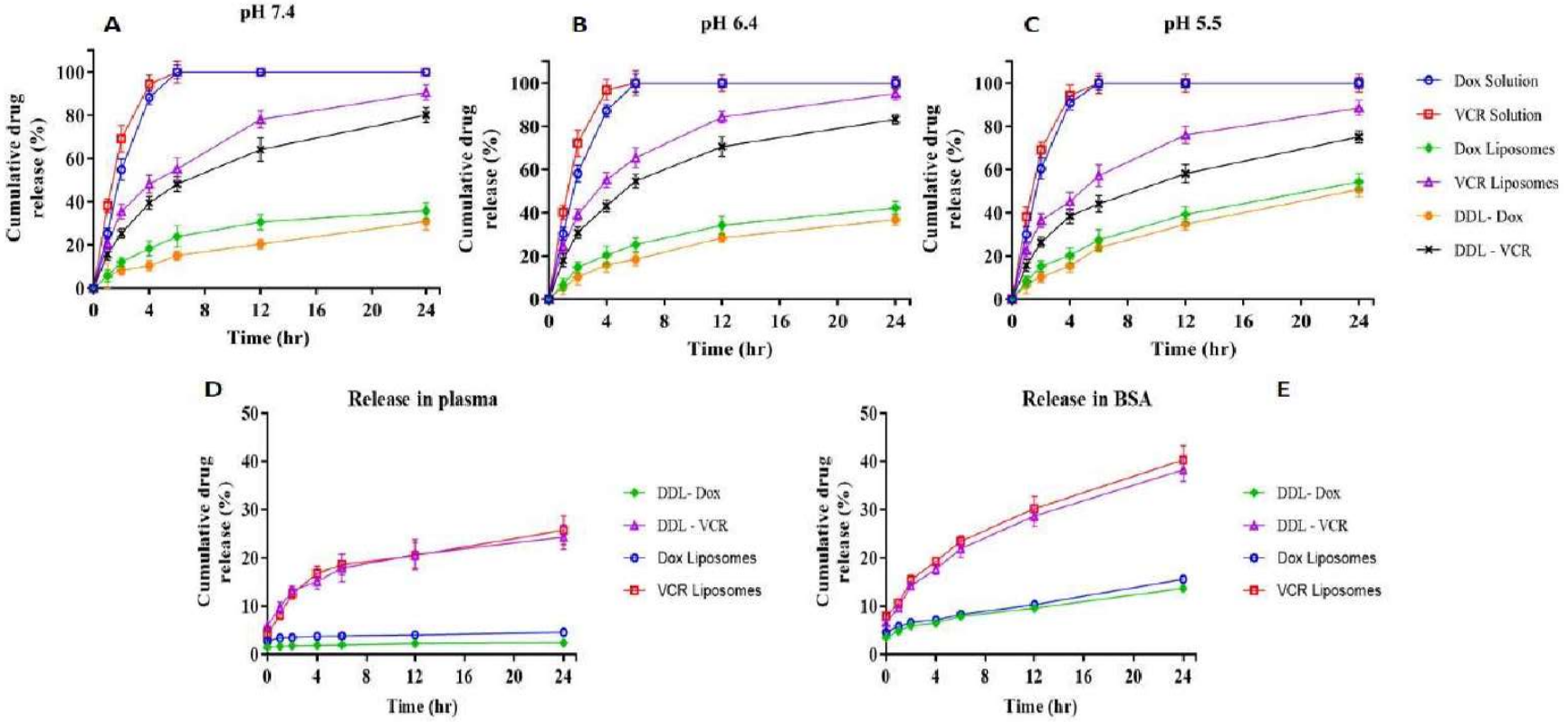

Figure 43: Release profile for drug solution, single and dual loaded liposomal formulations at pH 7.4 (A), pH 6.4 (B), pH 5.5 (C), on dilution with plasma (D), on dilution with bovine serum albumin (E).

8.4.15 Drug release kinetics study

The results of the in-vitro drug release were subsequently fitted into various drug release models (Zero Order, First Order, Higuchi, Korsmeyer Peppas, Hixon Crowell) to understand the release mechanism of both drugs under varying pH conditions from the liposomal formulations as well as to assessing the similarity of the drug release of the individual drugs from single and dual formulations. The release kinetics along with correlation coefficients (R^2) from the liposomal formulations are presented in Table 26. The aforementioned results of DOX release from both the liposomal formulations may be best explained by the Higuchi equation and Korsmeyer-Peppas equation at all the tested pH conditions. This indicates toward time-dependent fickinian diffusion-controlled release profile (Higuchi model) which may be attributed to the drug release from the precipitated doxorubicin sulphate nanocrystals. Additionally, the DOX release was also found to be erosion and diffusion controlled (Korsmeyer-Peppas) which may be attributed to the erosion of the lipid bilayer and the diffusion of DOX from the in-situ DOX sulphate though the eroded bilayer into the surrounding medium. VCR release from the liposomal formulations was found to be biphasic in nature with initial burst release followed by slow release of the drug through the lipid bilayer. VCR burst release was found to be best explained by concentration dependent first order kinetics which may be attributed to the soluble nature of the in-situ VCR sulphate inside the liposomes and its ability to cross the lipid bilayer. Additionally, the slow release may be explained by the Higuchi and the Korsmeyer-Peppas models indicating towards the presence of the erosion and diffusion-controlled mechanisms of VCR release. Since DOX and VCR release profiles and kinetics were found to be similar in dual drug liposomes as compared to single drug formulations, it may be inferred that the presence of additional drug in the liposomal carrier does not alter the individual drug release at the various pH conditions presented in-vivo to the liposomal formulations (40).

Similarly, the drug release in presence of serum was found to present time dependant fickinian diffusion-controlled release of both the drugs (Higuchi model). Drug release modelling in BSA indicated drug release of DOX to be limited by the dissolution velocity through the lipid bilayer (Hixon-Crowell) and being independent of the concertation of the drug (Zero order) while that

for VCR, it was diffusion-controlled process (Higuchi model) over the intended drug release period.

Further, the results for different pH conditions indicate that while DOX release is governed by diffusion-controlled mechanisms while VCR release is governed by both concentration dependent release and diffusion-controlled mechanisms. The difference in the release kinetics of the drugs from the liposomal formulations may be attributed to two factors: intrinsic solubility of the sulphate salts of the two drugs and their permeability across the lipid bilayer. These drug release profiles necessitate the evaluation of haemolysis potential of the optimized formulation to assess the in-vivo toxicity profile to the normal tissues.

pH	Kinetic model	DOX release		VCR release	
		DOX liposomes	Dual liposomes	VCR Liposomes	Dual liposomes
5.5	Zero Order	y = 2.0847x + 8.9885 R^2 = 0.9097	y = 2.0188x + 6.1198 R^2 = 0.9437	y = 3.1666x + 24.404 R^2 = 0.7794	y = 2.7238x + 17.774 R^2 = 0.8284
	First Order	y = -0.0135x + 1.9649 R^2 = 0.9654	y = -0.0125x + 1.9786 R^2 = 0.9809	y = -0.0375x + 1.9058 R^2 = 0.9664	y = -0.0234x + 1.9278 R^2 = 0.9559
	Higuchi	y = 11.405x - 1.2275 R^2 = 0.9961	y = 10.792x - 3.2229 R^2 = 0.9865	y = 18.421x + 6.4989 R^2 = 0.965	y = 15.515x + 3.0904 R^2 = 0.9834
	Korsmeyer Peppas	y = 0.575x + 0.9672 R^2 = 0.9884	y = 0.653x + 0.8242 R^2 = 0.9933	y = 0.426x + 1.3989 R^2 = 0.9755	y = 0.4779x + 1.2514 R^2 = 0.9755
	Hixon Crowell	y = -0.6949x + 30.337 R^2 = 0.9097	y = -0.6729x + 31.293 R^2 = 0.9437	y = -1.0555x + 25.199 R^2 = 0.7794	y = -0.9079x + 27.409 R^2 = 0.8284
6.4	Zero Order	y = 1.5905x + 9.4039 R^2 = 0.8245	y = 1.4215x + 6.5541 R^2 = 0.8875	y = 3.3794x + 28.293 R^2 = 0.7366	y = 3.0453x + 21.642 R^2 = 0.7828
	First Order	y = -0.0093x + 1.9582 R^2 = 0.8818	y = -0.0079x + 1.9721 R^2 = 0.9263	y = -0.0532x + 1.9056 R^2 = 0.9825	y = -0.031x + 1.9106 R^2 = 0.9471
	Higuchi	y = 9.0477x + 0.8562 R^2 = 0.9762	y = 7.8573x - 0.5874 R^2 = 0.9921	y = 20.01x + 8.4209 R^2 = 0.9448	y = 17.67x + 4.5225 R^2 = 0.9642
	Korsmeyer Peppas	y = 0.5526x + 0.9304 R^2 = 0.94	y = 0.58x + 0.8087 R^2 = 0.983	y = 0.4276x + 1.4453 R^2 = 0.9589	y = 0.478x + 1.3183 R^2 = 0.9627
	Hixon Crowell	y = -0.5302x + 30.199 R^2 = 0.8245	y = -0.4738x + 31.149 R^2 = 0.8875	y = -1.1265x + 23.902 R^2 = 0.7366	y = -1.0151x + 26.119 R^2 = 0.7828
7.4	Zero Order	y = 1.3539x + 8.5885 R^2 = 0.7803	y = 1.1629x + 4.8009 R^2 = 0.9331	y = 3.291x + 23.819 R^2 = 0.7886	y = 2.9841x + 18.094 R^2 = 0.8303

pH	Kinetic model	DOX release		VCR release	
		DOX liposomes	Dual liposomes	VCR Liposomes	Dual liposomes
	First Order	y = -0.0075x + 1.9611 R² = 0.8266	y = -0.0061x + 1.9801 R² = 0.9583	y = -0.0413x + 1.917 R² = 0.9756	y = -0.028x + 1.9313 R² = 0.9655
	Higuchi	y = 7.8293x + 1.035 R² = 0.9546	y = 6.2747x - 0.7076 R² = 0.9938	y = 19.055x + 5.4061 R² = 0.9673	y = 16.966x + 2.0775 R² = 0.9819
	Korsmeyer Peppas	y = 0.5656x + 0.8629 R² = 0.9258	y = 0.53x + 0.7449 R² = 0.9915	y = 0.4572x + 1.3742 R² = 0.9671	y = 0.5131x + 1.2442 R² = 0.9767
	Hixon Crowell	y = -0.4513x + 30.471 R² = 0.7803	y = -0.3876x + 31.733 R² = 0.9331	y = -1.097x + 25.394 R² = 0.7886	y = 0.5131x + 1.2442 R² = 0.9767
Drug release in plasma	Zero Order	y = 0.0589x + 3.3003 R² = 0.7956	y = 0.0345x + 1.6741 R² = 0.8386	y = 2.1171x + 13.705 R² = 0.8535	y = 1.9455x + 14.83 R² = 0.8275
	First Order	y = -0.0003x + 1.9854 R² = 0.7984	y = -0.0002x + 1.9927 R² = 0.8394	y = -0.0146x + 1.9409 R² = 0.9328	y = -0.0131x + 1.9331 R² = 0.9014
	Higuchi	y = 0.3382x + 2.9771 R² = 0.9585	y = 0.1948x + 1.492 R² = 0.9773	y = 11.811x + 2.8333 R² = 0.9718	y = 10.946x + 4.6381 R² = 0.9584
	Korsmeyer Peppas	y = 0.1162x + 0.4965 R² = 0.8227	y = 0.134x + 0.1979 R² = 0.9492	y = 0.7244x + 0.8943 R² = 0.8486	y = 0.6393x + 0.9707 R² = 0.8924
	Hixon Crowell	y = -0.0196x + 32.233 R² = 0.7956	y = -0.0115x + 32.775 R² = 0.8386	y = -0.7057x + 28.765 R² = 0.8535	y = -0.6485x + 28.39 R² = 0.8275
Drug release in bovine serum albumin	Zero Order	y = 0.4309x + 5.3148 R² = 0.9893	y = 0.39x + 4.7013 R² = 0.9607	y = 1.2883x + 11.99 R² = 0.9265	y = 1.2529x + 10.8 R² = 0.9248
	First Order	y = -0.0021x + 1.9765 R² = 0.9411	y = -0.0019x + 1.9792 R² = 0.9466	y = -0.0076x + 1.9465 R² = 0.957	y = -0.0072x + 1.9521 R² = 0.9543
	Higuchi	y = 2.2019x + 3.5418 R² = 0.9449	y = 2.0609x + 2.9485 R² = 0.9413	y = 6.9536x + 5.8828 R² = 0.9874	y = 6.7752x + 4.8321 R² = 0.9894
	Korsmeyer Peppas	y = 0.3181x + 0.7008 R² = 0.9332	y = 0.3554x + 0.6237 R² = 0.9392	y = 0.4616x + 0.9911 R² = 0.9606	y = 0.4885x + 0.9375 R² = 0.9464
	Hixon Crowell	y = -0.1436x + 31.562 R² = 0.9893	y = -0.13x + 31.766 R² = 0.9807	y = -0.4294x + 29.337 R² = 0.9265	y = -0.4176x + 29.733 R² = 0.9248

Table 26: DOX and VCR drug release kinetics from single drug loaded and dual loaded liposomal formulations

8.4.16 Haemolysis Study

The extent of physiological compatibility of the optimized formulation post administration into the blood was determined using in-vitro haemolysis study. This assessment of toxicity of formulations to RBC was conducted to evaluate the extent of membrane damage and rupture potential of erythrocytes while ascertaining the safety profile of the drug formulations in response to the varying in-vivo pH conditions. Results of haemolytic potential of free drug solutions, drug free liposomes, single drug loaded and dual drug loaded liposomes are presented in Figure 44. The optical microscope images of the erythrocytes incubated with the liposomal formulations after 0.5 hour (Figure 44 A-D) and 1 hour indicated the absence of haemolytic potential of these carriers (Figure 45i A-D). Further, the results exhibit a concentration dependent increase in haemolysis which was significantly increased for the drug solutions as compared to formulations and the drug free liposomes (placebo). These results of drug free liposomes indicate towards lack of haemolytic potential of the lipidic components used for formulating the liposomes which substantiates the clinically evident compatibility of liposome-based delivery of chemotherapeutic agents (41). Further, at highest concentration tested (5000µg/ml), VCR solution and DOX solution exhibited around 54% and 42% haemolysis respectively whereas the same was observed at significantly reduced levels for VCR liposomes, DOX liposomes and dual drug liposomes (3%, 0.8% and 0.9% respectively) (Figure 45ii). These results indicate towards high compatibility of the optimized formulation with the erythrocytes and this may be attributed to the encapsulation of both the drugs in the liposomal core leading to the absence of direct interaction potential with the erythrocyte membrane (42).

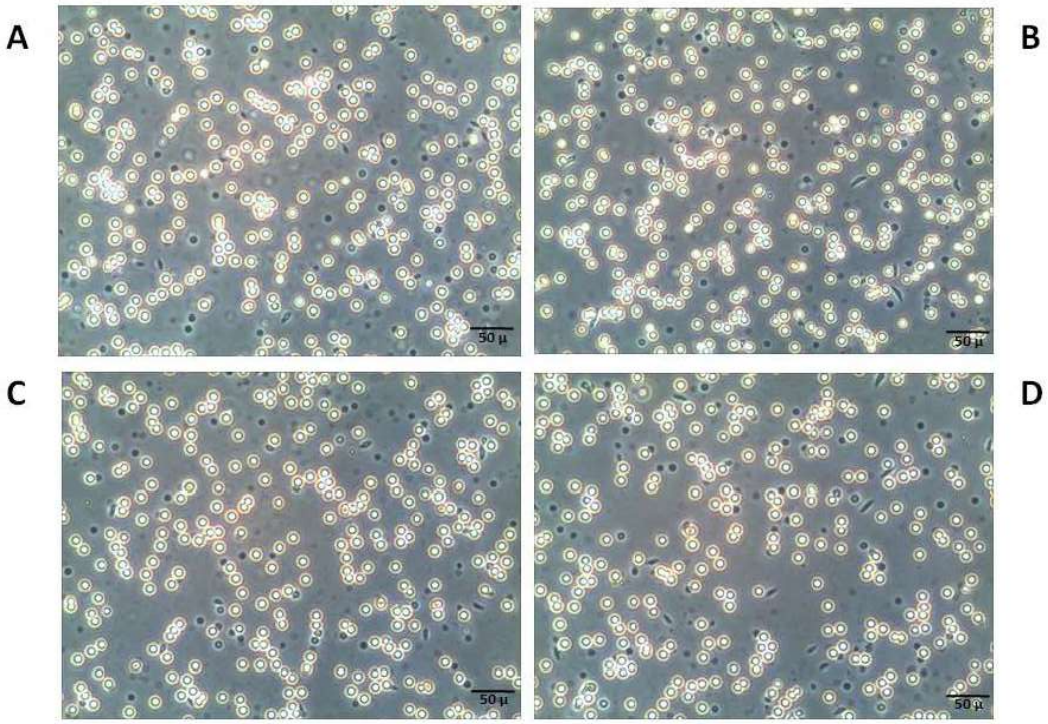

Figure 44: Optical microscopy images of formulation induced Haemolysis for various tested formulations at 0.5 hour at 500 µg/ml concentration of the drugs (A: Blank liposomes; B: Dox liposomes; C: VCR liposomes; D: Dual loaded liposomes).

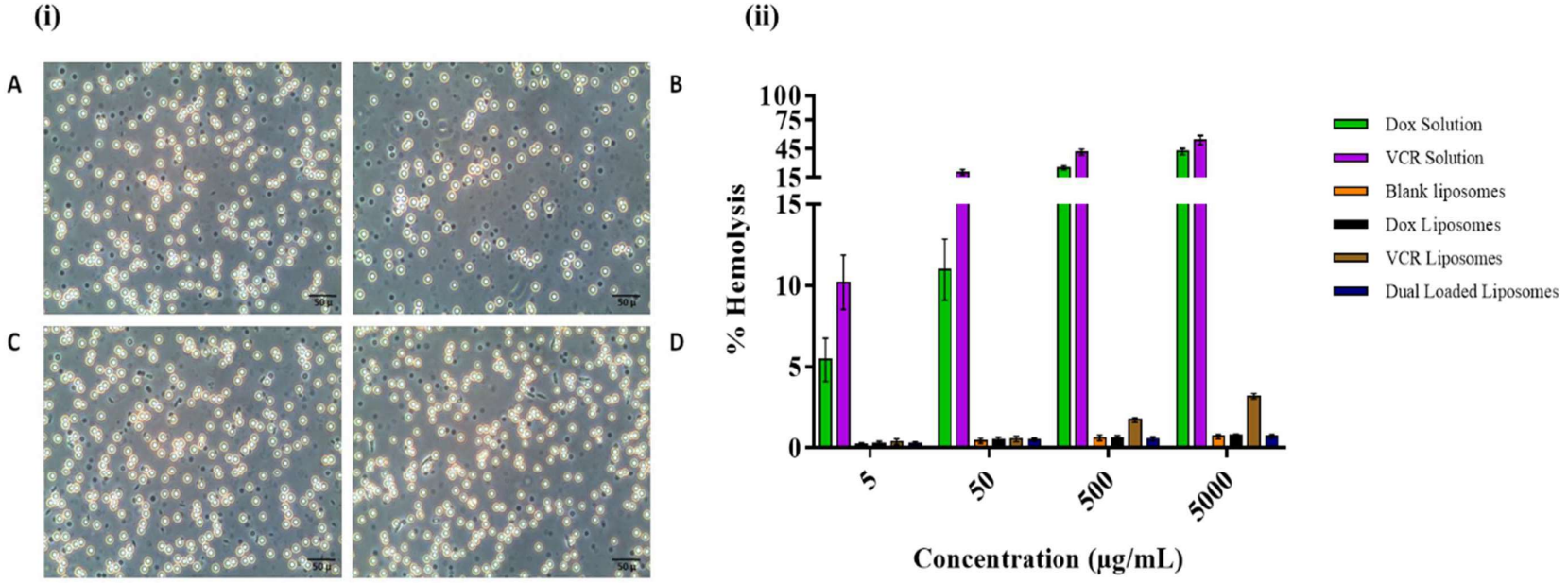

Figure 45: (i) Optical microscopy images of formulation induced Haemolysis for various tested formulations at one hour at 500 µg/ml concentration of the drugs (A: Blank liposomes; B: Dox liposomes; C: VCR liposomes; D: Dual loaded liposomes). (ii) % haemolysis for various carrier free drug solutions, drug free liposomes, single liposomes and dual liposomal formulations at varying concentrations.

8.4.17 Stability study

The optimized dual drug liposomal suspension was tested for physico-chemical stability at storage conditions of 2-8°C for 12 months and 25°C /60% RH for 1 month in stoppered and sealed 10 ml clear colourless tubular USP-type I glass vials. The stability study was performed to evaluate the impact of storage at various conditions on the assay and free drug of both drugs, particle size and zeta potential as well as to determine the shelf life of the formulation. The results of the evaluated parameters as a function of time are presented in Table 27 ad Figures 46-48. The results indicate that no significant change was observed in all the tested parameters when stored at 2-8°C indicating towards the intrinsic stability of the formulation in the suspension state at this temperature for atleast 12 months. However, significant changes ($p<0.05$) were observed in the tested parameters on storage at 25°C /60% RH for 1 month which is inline results of the commercially available liposomal doxorubicin formulations (43). The decrease in the assay and increase in free drug content of both drugs may be attributed to temperature induced degradation of the active molecules and lipid bilayer when present in solution state. The decrease in the zeta potential may be attributed to increased free drug content while increase in the particle size may be due to the lipid degradation (44). Importantly, the optimized formulation may be stored in suspension state at 2-8°C for the experimentally determined shelf life of 12 months and predicted shelf life of 18 months (determined using Minitab software with 10% free drug of VCR as the determinant at 95% CI and $\alpha=0.05$) without lyophilization of the sample (45).

Storage conditions	Vincristine content		Doxorubicin content		Particle Size (PDI)		Zeta Potential (mV)
	Assay (%)	Free drug (%)	Assay (%)	Free drug (%)	Particle size (nm)	PDI	
0 M	98.91± 2.13	5.97± 1.12	99.61± 1.21	3.96± 1.07	98.74± 2.42	0.058	-7.89± 1.21
3 M, 2-8°C	97.73± 2.5	6.31± 0.89	98.51± 1.77	4.12±0.91	97.95± 4.08	0.068	-7.81±1.59
6 M, 2-8°C	96.18± 1.95	6.87± 1.17	98.26± 1.98	4.27± 0.85	101.42± 2.81	0.065	-8.21±2.37
9 M, 2-8°C	95.59± 2.86	7.12± 0.75	97.31± 2.57	4.51± 0.95	99.59± 4.17	0.074	-7.95±1.96
12M, 2-8°C	95.01± 2.71	7.15± 1.28	97.17±1.95	4.86± 1.01	100.71± 3.95	0.081	-7.78±2.13
1M, 25°C	75.21± 5.82	15.31± 3.41	85.16± 2.17	12.58± 2.51	105.86± 5.32	0.132	-3.61±2.86

Table 27: Results of assay, free drug of VCR and DOX; particle size, zeta potential of optimized dual drug formulation on storage at 2-8 ˚C and 25˚C. Results of the study are presented as mean ± SD (n=3).

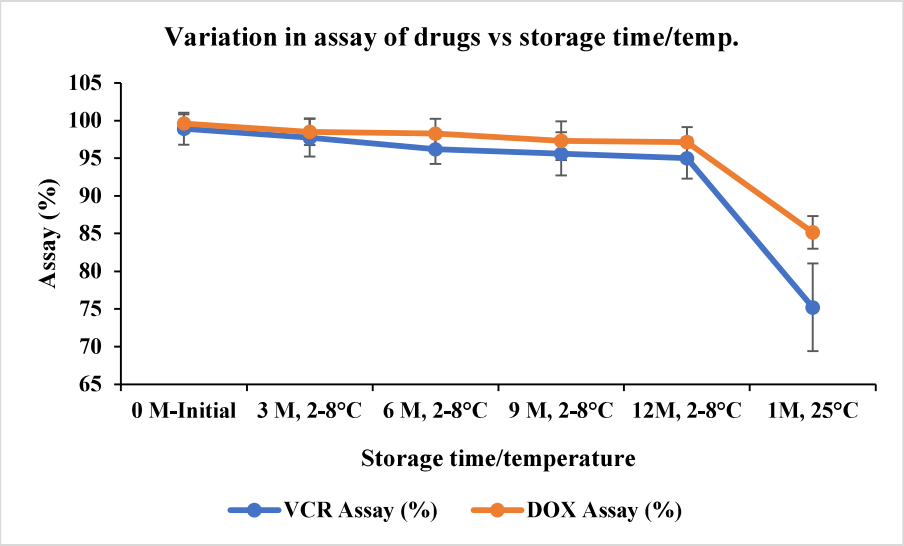

Figure 46: Stability study: variation in the assay of the drugs (DOX, VCR) with storage at temperature (2-8°C and 25±2°C/65±5%RH) with time

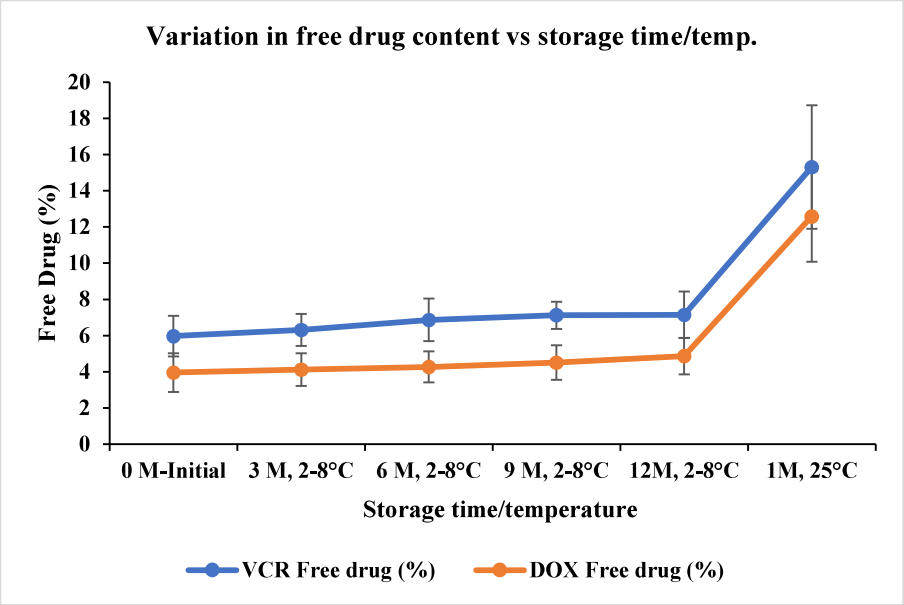

Figure 47: Stability study: variation in the free drug content (DOX, VCR) with storage at temperature (2-8°C and 25±2°C/65±5%RH) with time

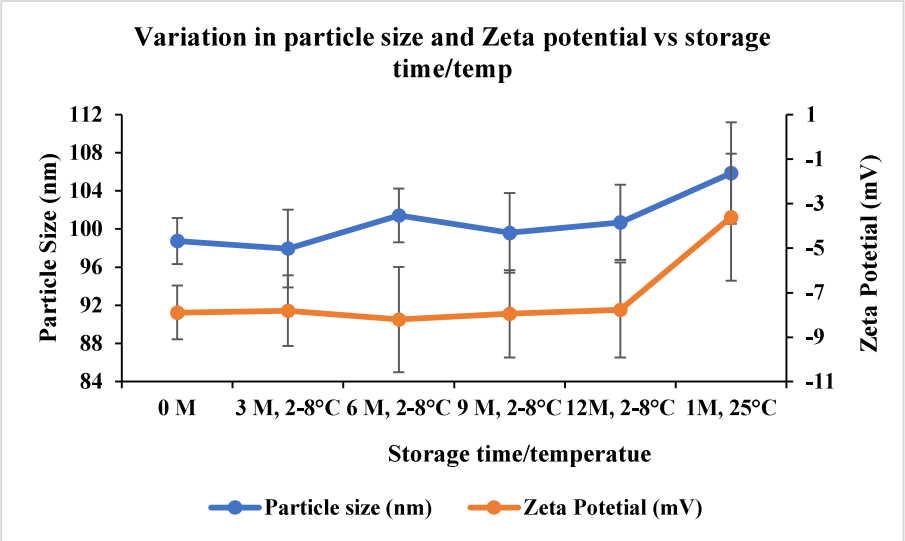

Figure 48: Stability study: variation in the particle size and zeta potential with storage at temperature (2-8°C and 25±2°C/65±5%RH) with time

8.5 Conclusion

The current section aimed at investigating the physicochemical and biochemical characteristics of the optimized dual drug liposome post co-encapsulation of synergistic ratio of the two drugs (doxorubicin and vincristine) in an optimized liposomal formulation. The optimized liposomal formulation presented non-significant difference in physicochemical and biochemical characteristics and stability as compared commercially available liposomal doxorubicin hydrochloride (clinical standard). Additionally, the newly formulated liposomal suspension was predicted to present 18M stability similar to approved product besides presenting with ease in scalability for manufacturing.

8.6 References

1. Barenholz YC. Doxil®—the first FDA-approved nano-drug: lessons learned. Journal of controlled release. 2012;160(2):117-34.

2. Maiti K, Bhowmick S, Jain P, Zope M, Doshi K, Rajamannar T. Comparison of Physicochemical Properties of Generic Doxorubicin HCl Liposome Injection with the Reference Listed Drug. Anti-cancer agents in medicinal chemistry. 2018;18(4):597-609.

3. Ghosh S, Mukherjee B, Chaudhuri S, Roy T, Mukherjee A, Sengupta S. Methotrexate aspasomes against rheumatoid arthritis: optimized hydrogel loaded liposomal formulation with in vivo evaluation in Wistar rats. AAPS PharmSciTech. 2018;19(3):1320-36.

4. Banerjee S, Pal TK, Guha SK. Probing molecular interactions of poly (styrene-co-maleic acid) with lipid matrix models to interpret the therapeutic potential of the co-polymer. Biochimica et Biophysica Acta (BBA)-Biomembranes. 2012;1818(3):537-50.

5. Paul P, Sengupta S, Mukherjee B, Shaw TK, Gaonkar RH, Debnath MC. Chitosan-coated nanoparticles enhanced lung pharmacokinetic profile of voriconazole upon pulmonary delivery in mice. Nanomedicine : nanotechnology, biology, and medicine. 2018;13(5):501-20.

6. Ghosh S, Mondal L, Chakraborty S, Mukherjee B. Early Stage HIV Management and Reduction of Stavudine-Induced Hepatotoxicity in Rats by Experimentally Developed Biodegradable Nanoparticles. AAPS PharmSciTech. 2017;18(3):697-709.

7. Shimada K, Miyagishima A, Sadzuka Y, Nozawa Y, Mochizuki Y, Ohshima H, et al. Determination of the thickness of the fixed aqueous layer around polyethyleneglycol-coated liposomes. Journal of drug targeting. 1995;3(4):283-9.

8. Sangrà M, Estelrich J, Sabaté R, Espargaró A, Busquets M. Evidence of protein adsorption in pegylated liposomes: influence of liposomal decoration. Nanomaterials. 2017;7(2):37.

9. Foteini P, Pippa N, Naziris N, Demetzos C. Physicochemical study of the protein-liposome interactions: influence of liposome composition and concentration on protein binding. Journal of liposome research. 2019:1-9.

10. Caracciolo G, Palchetti S, Digiacomo L, Chiozzi RZ, Capriotti AL, Amenitsch H, et al. Human biomolecular corona of liposomal doxorubicin: The overlooked factor in anticancer drug delivery. ACS applied materials & interfaces. 2018;10(27):22951-62.

11. Wibroe PP, Ahmadvand D, Oghabian MA, Yaghmur A, Moghimi SM. An integrated assessment of morphology, size, and complement activation of the PEGylated liposomal doxorubicin products Doxil®, Caelyx®, DOXOrubicin, and SinaDoxosome. Journal of Controlled Release. 2016;221:1-8.

12. Jiang W, Lionberger R, Yu LX. In vitro and in vivo characterizations of PEGylated liposomal doxorubicin. Bioanalysis. 2011;3(3):333-44.

13. Fatouros D, Hatzidimitriou K, Antimisiaris S. Liposomes encapsulating prednisolone and prednisolone–cyclodextrin complexes: comparison of membrane integrity and drug release. European journal of pharmaceutical sciences. 2001;13(3):287-96.

14. Rathore YS, Dhoke RR, Badmalia M, Sagar A. SAXS data based global shape analysis of Trigger Factor (TF) proteins from E. coli, V. cholerae, and P. frigidicola: resolving the debate on the nature of monomeric and dimeric forms. The Journal of Physical Chemistry B. 2015;119(20):6101-12.

15. Franke D, Petoukhov M, Konarev P, Panjkovich A, Tuukkanen A, Mertens H, et al. ATSAS 2.8: a comprehensive data analysis suite for small-angle scattering from macromolecular solutions. Journal of applied crystallography. 2017;50(4):1212-25.

16. Bhatt P, Lalani R, Vhora I, Patil S, Amrutiya J, Misra A, et al. Liposomes encapsulating native and cyclodextrin enclosed paclitaxel: Enhanced loading efficiency and its pharmacokinetic evaluation. International Journal of Pharmaceutics. 2018;536(1):95-107.

17. Utreja P, Jain S, Tiwary A. Localized delivery of paclitaxel using elastic liposomes: formulation development and evaluation. Drug delivery. 2011;18(5):367-76.

18. Cui J, Li C, Wang C, Li Y, Zhang L, Zhang L, et al. Development of pegylated liposomal vincristine using novel sulfobutyl ether cyclodextrin gradient: is improved drug retention sufficient to surpass DSPE-PEG-induced drug leakage? Journal of pharmaceutical sciences. 2011;100(7):2835-48.

19. Kannan V, Balabathula P, Thoma LA, Wood GC. Effect of sucrose as a lyoprotectant on the integrity of paclitaxel-loaded liposomes during lyophilization. Journal of liposome research. 2015;25(4):270-8.

20. Ewing AV, Biggart GD, Hale CR, Clarke GS, Kazarian SG. Comparison of pharmaceutical formulations: ATR-FTIR spectroscopic imaging to study drug-carrier interactions. International journal of pharmaceutics. 2015;495(1):112-21.

21. Zucker D, Marcus D, Barenholz Y, Goldblum A. Liposome drugs' loading efficiency: a working model based on loading conditions and drug's physicochemical properties. Journal of controlled release : official journal of the Controlled Release Society. 2009;139(1):73-80.

22. Chen W, Duša F, Witos J, Ruokonen S-K, Wiedmer SK. Determination of the main phase transition temperature of phospholipids by nanoplasmonic sensing. Scientific reports. 2018;8(1):14815.

23. Wei X, Cohen R, Barenholz Y. Insights into composition/structure/function relationships of Doxil® gained from "high-sensitivity" differential scanning calorimetry. European Journal of Pharmaceutics and Biopharmaceutics. 2016;104:260-70.

24. Cui J, Li C, Wang C, Li Y, Zhang L, Zhang L, et al. Development of pegylated liposomal vincristine using novel sulfobutyl ether cyclodextrin gradient: is improved drug retention sufficient to surpass DSPE–PEG-induced drug leakage? Journal of pharmaceutical sciences. 2011;100(7):2835-48.

25. Zucker D, Barenholz Y. Optimization of vincristine–topotecan combination—Paving the way for improved chemotherapy regimens by nanoliposomes. Journal of Controlled Release. 2010;146(3):326-33.

26. Banerjee P, Geng T, Mahanty A, Li T, Zong L, Wang B. Integrating the drug, disulfiram into the vitamin E-TPGS-modified PEGylated nanostructured lipid carriers to synergize its repurposing for anti-cancer therapy of solid tumors. International journal of pharmaceutics. 2019;557:374-89.

27. Burade V, Bhowmick S, Maiti K, Zalawadia R, Ruan H, Thennati R. Lipodox®(generic doxorubicin hydrochloride liposome injection): in vivo efficacy and bioequivalence versus Caelyx®(doxorubicin hydrochloride liposome injection) in human mammary carcinoma (MX-1) xenograft and syngeneic fibrosarcoma (WEHI 164) mouse models. BMC cancer. 2017;17(1):405.

28. Suk JS, Xu Q, Kim N, Hanes J, Ensign LM. PEGylation as a strategy for improving nanoparticle-based drug and gene delivery. Advanced drug delivery reviews. 2016;99:28-51.

29. Wolfram J, Suri K, Yang Y, Shen J, Celia C, Fresta M, et al. Shrinkage of pegylated and non-pegylated liposomes in serum. Colloids and Surfaces B: Biointerfaces. 2014;114:294-300.

30. Ishida T, Atobe K, Wang X, Kiwada H. Accelerated blood clearance of PEGylated liposomes upon repeated injections: effect of doxorubicin-encapsulation and high-dose first injection. Journal of controlled release. 2006;115(3):251-8.

31. Bonté F, Juliano R. Interactions of liposomes with serum proteins. Chemistry and physics of lipids. 1986;40(2-4):359-72.

32. Di Cola E, Grillo I, Ristori S. Small angle X-ray and neutron scattering: powerful tools for studying the structure of drug-loaded liposomes. Pharmaceutics. 2016;8(2):10.

33. Rieker T, Hanprasopwattana A, Datye A, Hubbard P. Particle size distribution inferred from small-angle X-ray scattering and transmission electron microscopy. Langmuir. 1999;15(2):638-41.

34. Grant TD, Luft JR, Carter LG, Matsui T, Weiss TM, Martel A, et al. The accurate assessment of small-angle X-ray scattering data. Acta Crystallographica Section D: Biological Crystallography. 2015;71(1):45-56.

35. Grunder R, Urban G, Ballauff M. Small-angle x-ray analysis of latex particles with core-shell morphology. Colloid and Polymer Science. 1993;271(6):563-72.

36. Kikhney AG, Svergun DI. A practical guide to small angle X-ray scattering (SAXS) of flexible and intrinsically disordered proteins. FEBS letters. 2015;589(19 Pt A):2570-7.

37. Fugit KD, Xiang TX, Choi du H, Kangarlou S, Csuhai E, Bummer PM, et al. Mechanistic model and analysis of doxorubicin release from liposomal formulations. Journal of controlled release : official journal of the Controlled Release Society. 2015;217:82-91.

38. Noble CO, Guo Z, Hayes ME, Marks JD, Park JW, Benz CC, et al. Characterization of highly stable liposomal and immunoliposomal formulations of vincristine and vinblastine. Cancer chemotherapy and pharmacology. 2009;64(4):741-51.

39. Ghosh S, Lalani R, Patel V, Bardoliwala D, Maiti K, Banerjee S, et al. Combinatorial nanocarriers against drug resistance in hematological cancers: Opportunities and emerging strategies. Journal of controlled release : official journal of the Controlled Release Society. 2019;296:114-39.

40. Jain A, Jain SK. In vitro release kinetics model fitting of liposomes: An insight. Chemistry and physics of lipids. 2016;201:28-40.

41. Cedrone E, Neun B, Rodriguez J, Vermilya A, Clogston J, McNeil S, et al. Anticoagulants influence the performance of in vitro assays intended for characterization of nanotechnology-based formulations. Molecules. 2018;23(1):12.

42. Jumaa M, Müller BW. Lipid emulsions as a novel system to reduce the hemolytic activity of lytic agents: mechanism of the protective effect. European journal of pharmaceutical sciences. 2000;9(3):285-90.

43. Allen TM, Cullis PR. Liposomal drug delivery systems: from concept to clinical applications. Advanced drug delivery reviews. 2013;65(1):36-48.

44. Payton NM, Wempe MF, Xu Y, Anchordoquy TJ. Long-term storage of lyophilized liposomal formulations. Journal of pharmaceutical sciences. 2014;103(12):3869-78.

45. Franzé S, Selmin F, Samaritani E, Minghetti P, Cilurzo F. Lyophilization of liposomal formulations: still necessary, still challenging. Pharmaceutics. 2018;10(3):139.